

PhD Defense

Reliability-based topology optimization frameworks for the design of structures subjected to random excitations

Junho Chun

Department of Civil and Environmental Engineering
University of Illinois, Urbana-Champaign
June 15th, 2016

Committee Members:

Glaucio H. Paulino, PhD
Junho Song, PhD
Ahmed E. Elbanna, PhD
Ivan F. M. Menezes, PhD
Andrés Tovar, PhD
William F. Baker, SE, FASCE



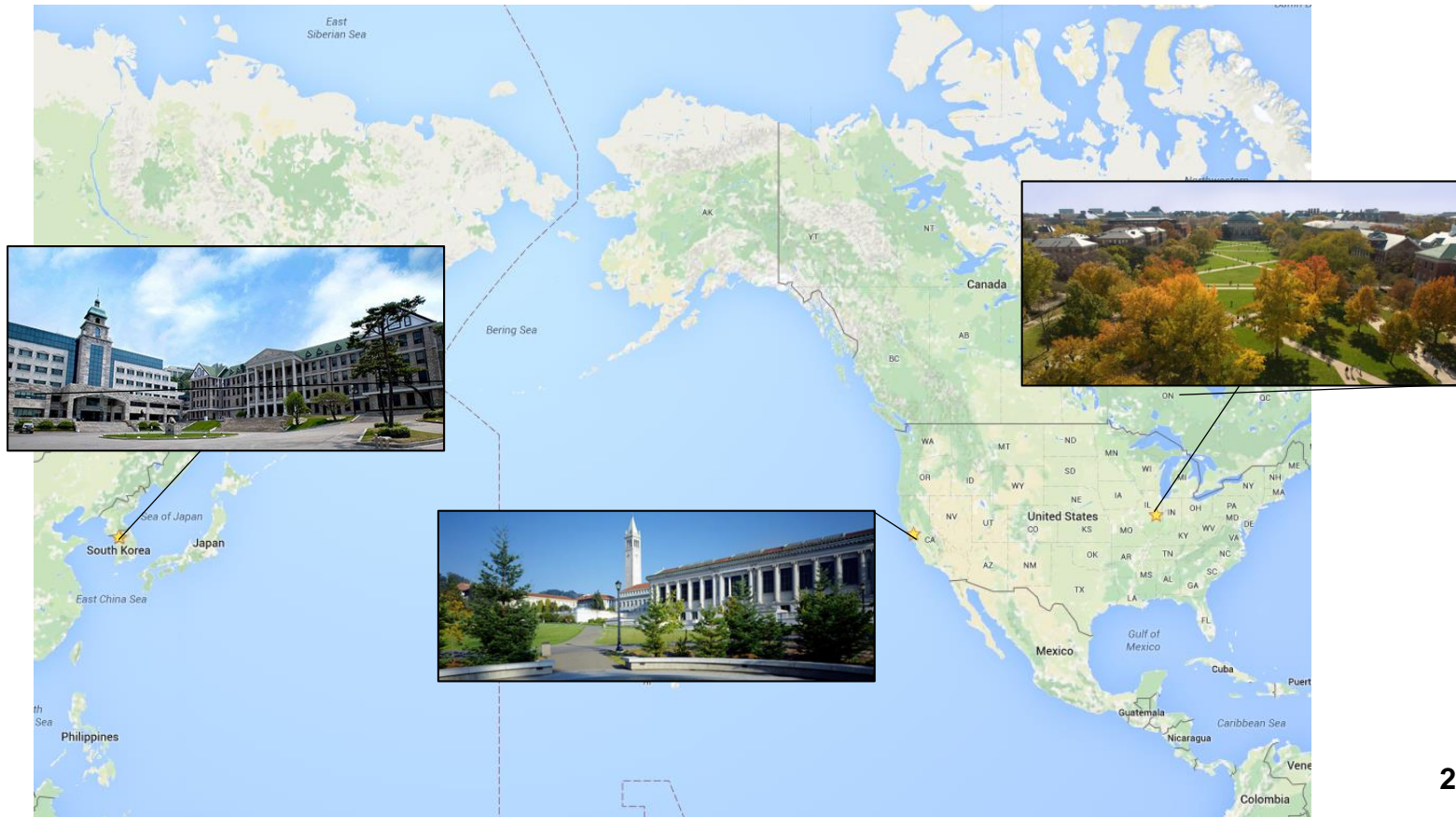
Educational background

Education

B.S (2006, Architectural Engineering), *Hanyang University*, Seoul, Korea

M.S (2007, Structural Engineering), *University of California, Berkeley*, CA

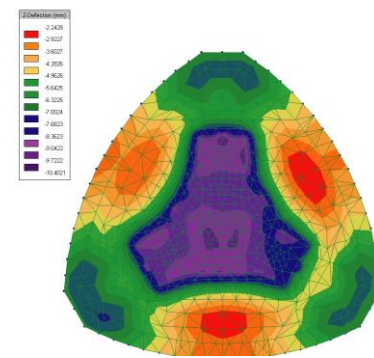
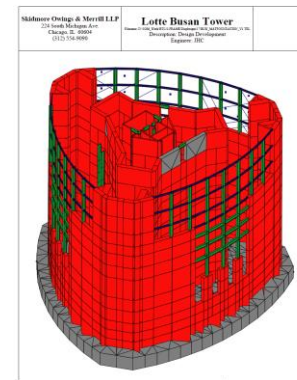
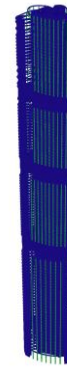
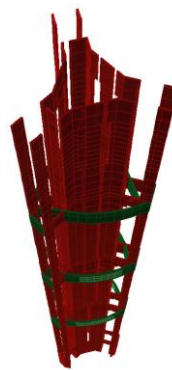
Ph.D (2010-present, Structural Engineering), *University of Illinois, Urbana-Champaign*, IL. **Advisors:** Glaucio H. Paulino, Junho Song



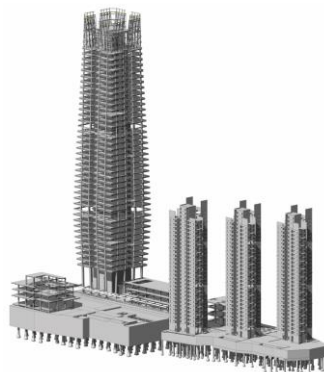
Professional background

Professional experience

Skidmore, Owings, & Merrill LLP, Chicago, IL, USA
Structural Engineer (September 2007 - June 2010)



Busan lotter tower (Courtesy of Skidmore, Owings & Merrill, LLP)



China merchant (Courtesy of Skidmore, Owings & Merrill, LLP)

Nanchang Greenland (Courtesy of Skidmore, Owings & Merrill, LLP)

Contributions

Discussed in this presentation:

Chun, J., Song, J., Paulino, G.H. (2015). Parameter sensitivity of system reliability using sequential compounding method. *Structural safety*, 55: 26–36. (**Chapter 4**)

Chun, J., Song, J., Paulino, G.H. System reliability-based design/topology optimization of structures constrained by first passage probability. To be submitted for journal publication. (**Chapter 5**)

Chun, J., Paulino, G.H, Song, J. Reliability-based topology optimization of truss structures using a discrete filtering technique. To be submitted for journal publication. (**Chapter 6**)

Not covered in this presentation:

Filipov*, E.T., **Chun***, J., Paulino, G.H., Song, J. (2016). Polygonal multiresolution topology optimization (PolyMTOP) for structural dynamics. *Structural and Multidisciplinary Optimization*, 53(4): 673-694. (**Chapter 2**)

Chun, J., Song, J., Paulino, G.H. (2016). Structural topology optimization under constraints on instantaneous failure probability. *Structural and Multidisciplinary Optimization*. 53(4): 773-799. (**Chapter 3**)

Structural engineering under natural hazards and risks

One of the most **fundamental requirements** on building structures is to **withstand** various **uncertain loads**.

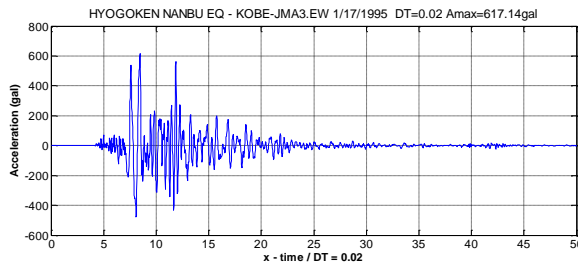


San Francisco Earthquake, 1906



Kobe Earthquake, 1995

The structural design needs to ensure **safe** and **reliable operations** over a prolonged period of time despite random excitations caused by hazardous events.



Random Excitations

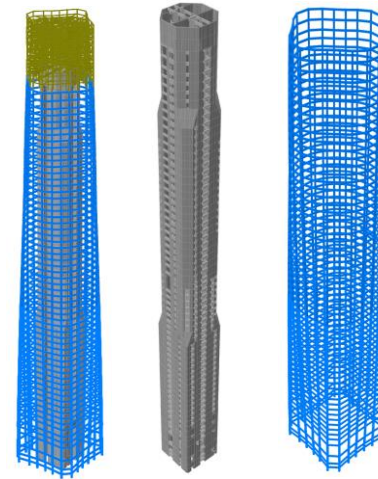
- Random processes
- Non-deterministic excitations
- Many possibilities of the process

Research aim: identification of the optimal structure and system under dynamic and stochastic excitations

Structural Design

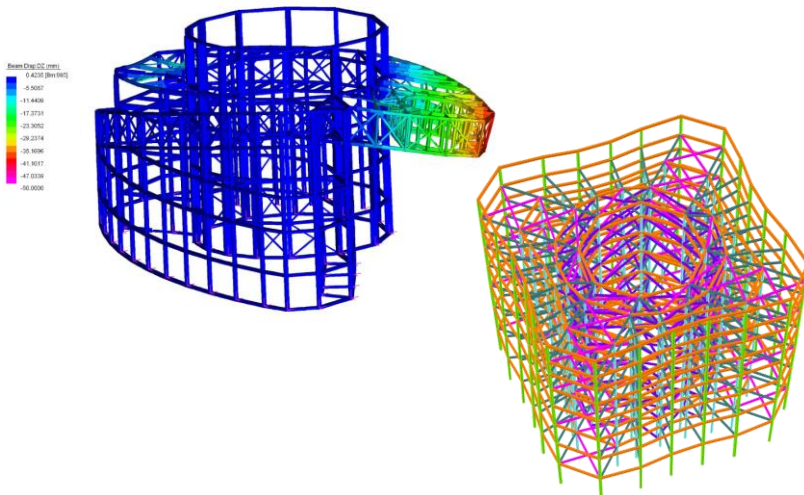


Courtesy of Skidmore, Owing and Merrill, LLP

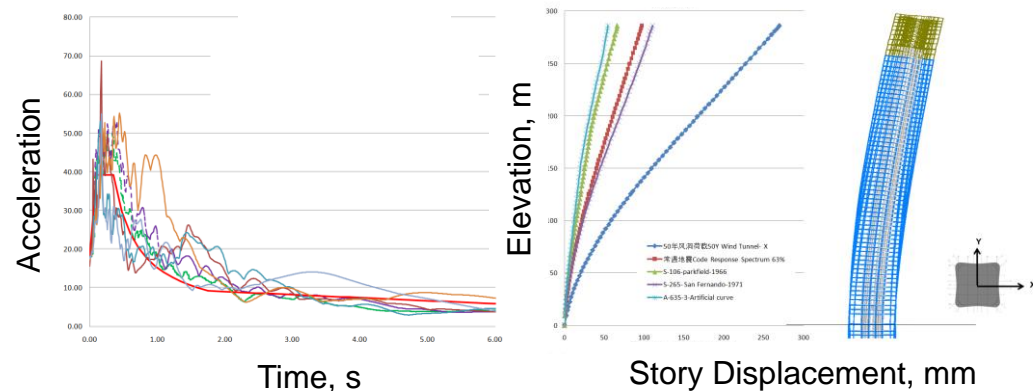


Structural system

Structural elements optimization

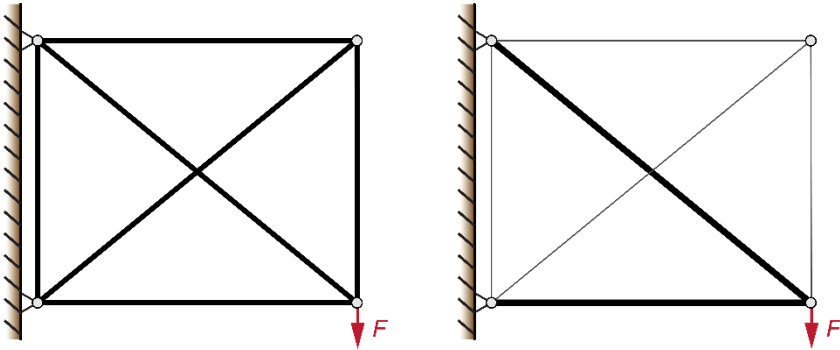


Structural performance optimization



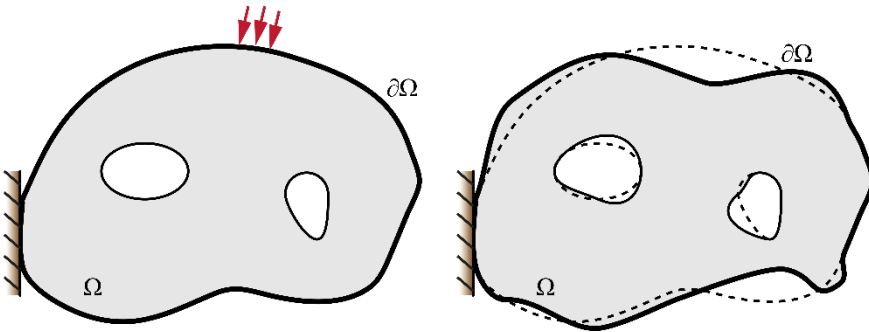
Categorization of structural optimization

Size Optimization

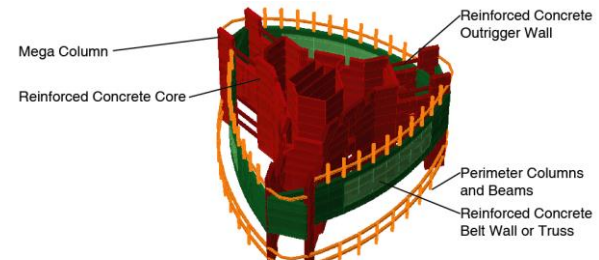
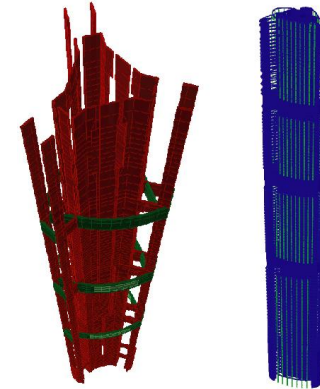


Design variable, d : **area**

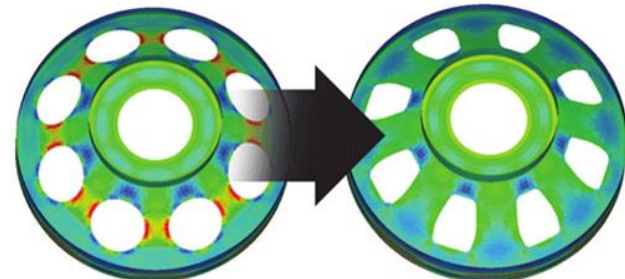
Shape Optimization



Design variable, d : **boundary** of shape



Courtesy of Skidmore, Owing and Merrill, LLP



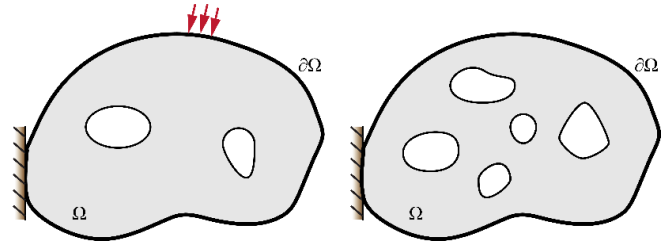
<http://www.altairhyperworks.com/>

Initial design Optimized design

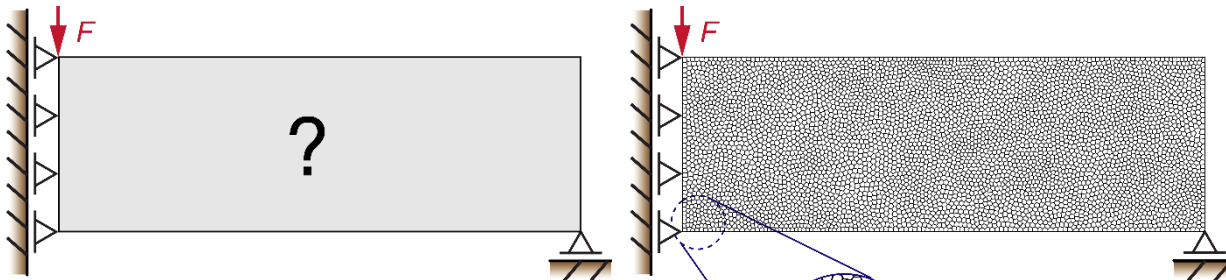
Stress contour

Categorization of structural optimization

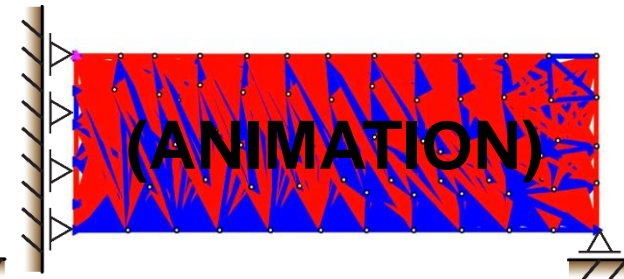
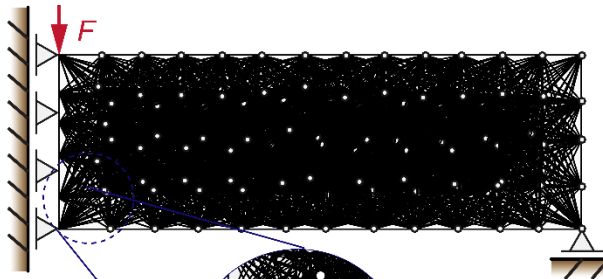
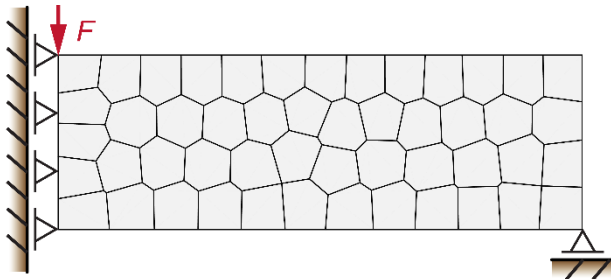
Topology Optimization: Continuum Design variable, d : density



$$\begin{array}{ll} \max_d & \text{stiffness} \\ \text{s.t} & \text{volume fraction} \end{array}$$



Topology Optimization: Ground structure Design variable, d : area



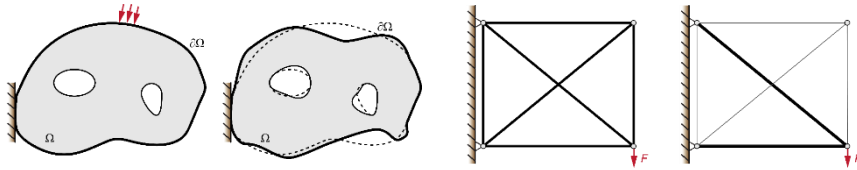
Design variable, d : area

$$0 \leq \rho_e \leq 1 \quad \begin{cases} \rho_e = 0 & \text{void} \\ \rho_e = 1 & \text{solid} \end{cases}$$

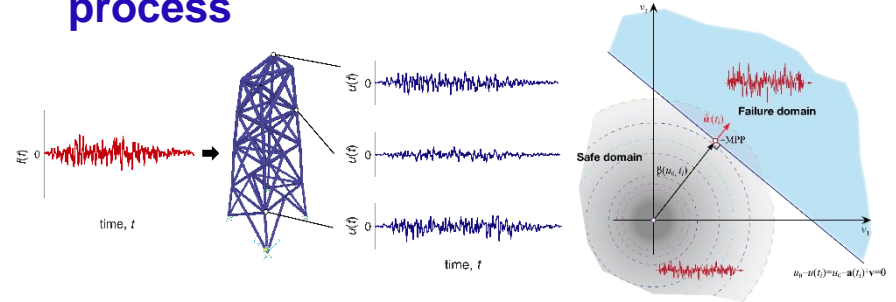
$$\mathbf{K}^e(\rho_e) = \rho_e^p \int_{\Omega_e} \mathbf{B}^T \mathbf{D}_0 \mathbf{B} \, \Omega_e$$

Presentation outline

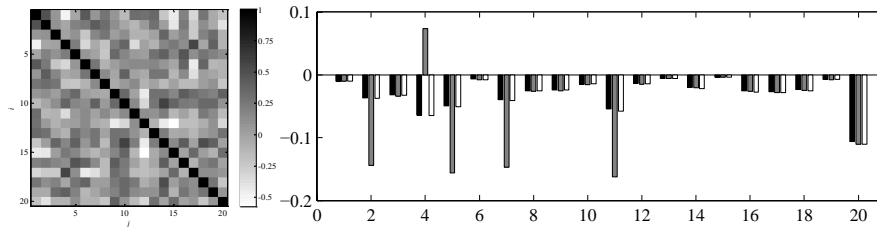
1. Introduction



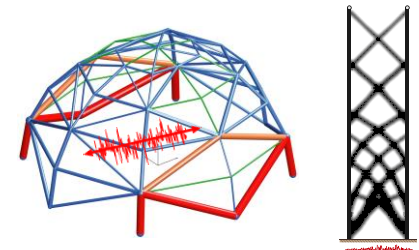
2. Discrete representation of stochastic process



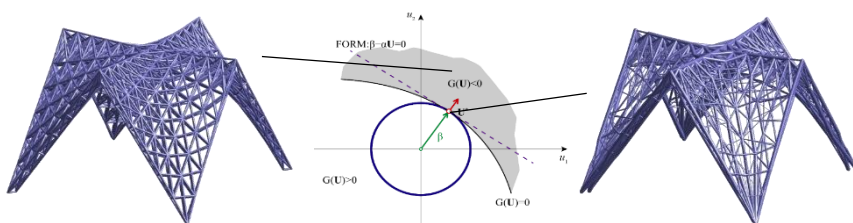
3. Parameter sensitivity of system reliability



4. Structural design and topology optimization under stochastic excitations



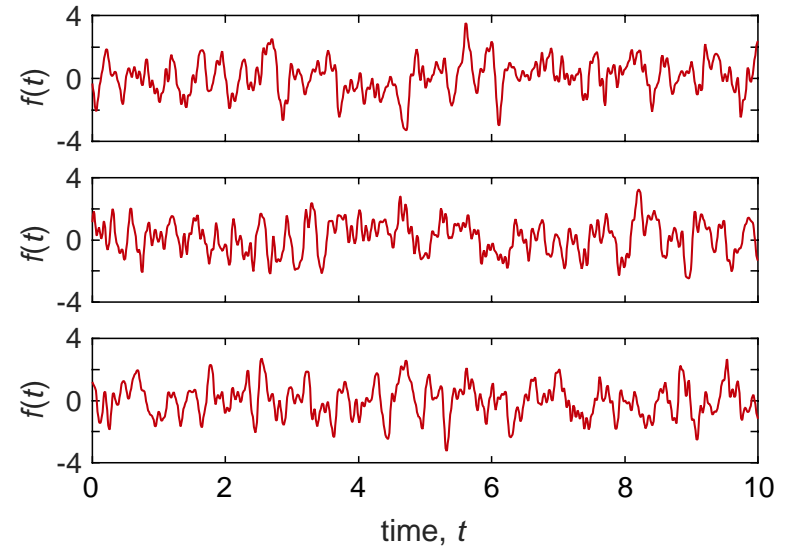
5. Reliability-based topology optimization by ground structure method



Reasonable representation of the random process is needed to obtain a meaningful solution

Stochastic excitation is often described by a random process

Random process can be understood as a collection of random variables defined along the time axis



□ Discrete Representation of Stochastic Excitation

The **stochastic excitation** is represented by a linear combination of **basis functions**, $s(t)$, with standard normal **independent random variables**, \mathbf{v} :

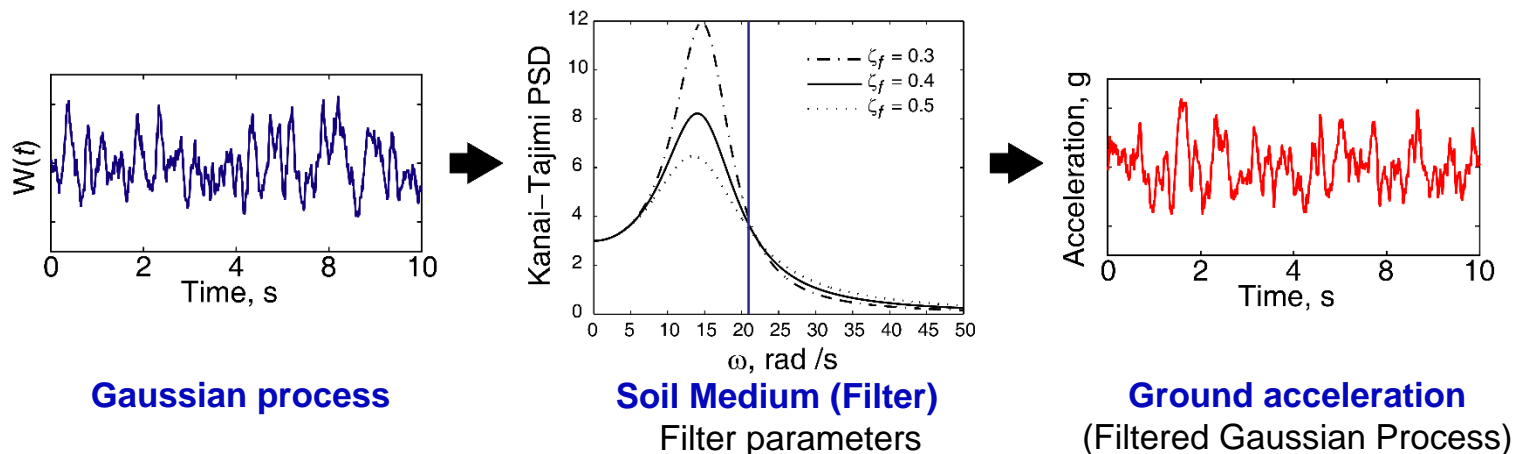
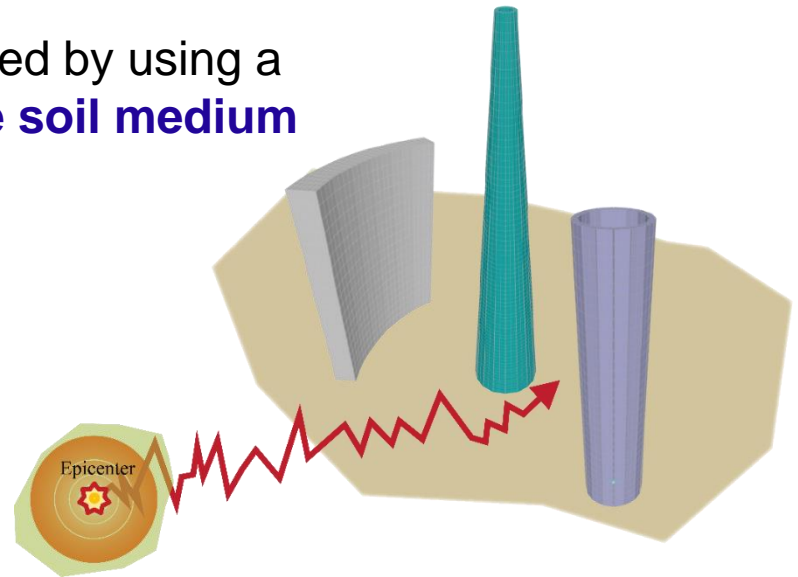
$$f(t) = \mu(t) + \sum_{i=1}^n v_i s_i(t) = \mu(t) + \mathbf{s}(t)^T \mathbf{v}$$

Stochastic ground motion is modeled as the response of a linear filter to a random pulse train

□ Modeling Ground Excitations - Filtered Gaussian Process

Stochastic ground excitations can be modeled by using a **filter** representing the **characteristic of the soil medium** and Gaussian process.

$$\begin{aligned}
 f(t) &= \int_0^t W(\tau) h_f(t - \tau) d\tau \\
 &\cong \sum_{i=1}^n W_i \cdot h_f(t - t_i) \Delta t \\
 &= \sum_{i=1}^n \sqrt{2\pi\Phi_0 / \Delta t} \cdot v_i \cdot h_f(t - t_i) \Delta t = \mathbf{s}(t)^T \mathbf{v}
 \end{aligned}$$

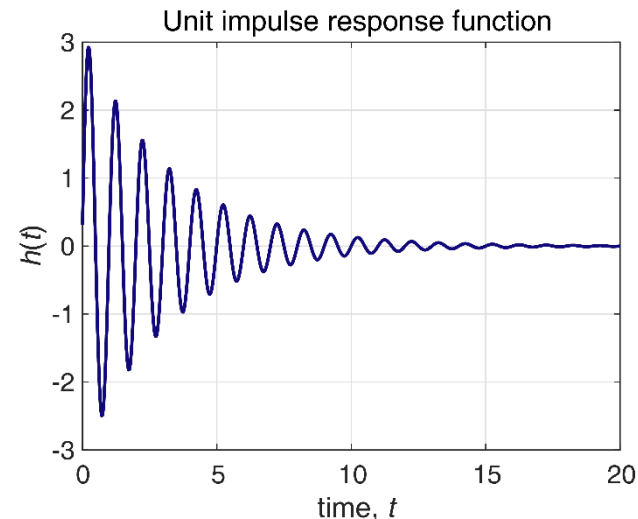
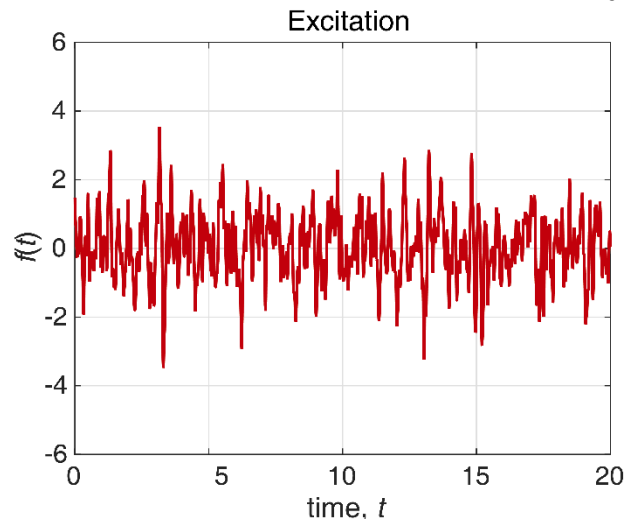


Stochastic response of a structure is described by a finite number of random variables

□ Dynamic Response

Convolution integral for responses of linear systems subjected to the stationary process can be developed with the impulse response function.

$$u(t) = \int_0^t f(\tau) h_s(t - \tau) d\tau$$



$$u(t) = \int_0^t \sum_{i=1}^n v_i s_i(\tau) h_s(t - \tau) d\tau = \sum_{i=1}^n v_i a_i(t) = \mathbf{a}(t)^T \mathbf{v}$$

$$a_i(t) = \int_0^t s_i(\tau) h_s(t - \tau) d\tau, \quad i = 1, \dots, n$$

Deterministic, time-dependent
- filter + structure

Random, time-independent

Failure event is defined in terms of dynamic response in discretization representation form

Instantaneous Failure Probability

Failure event of a linear system at a certain time t_i is defined as

$$E_f : g(t_i, u_0) \leq 0 \equiv E_f : u(t_i) \geq u_0 \equiv E_f : \mathbf{a}(t_i)^\top \mathbf{v} \geq u_0$$

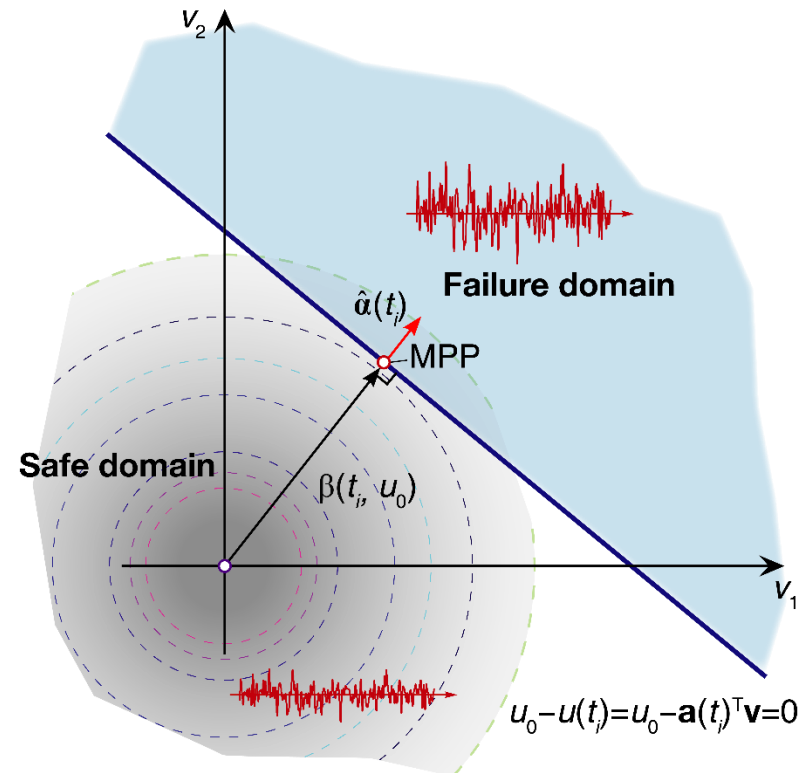
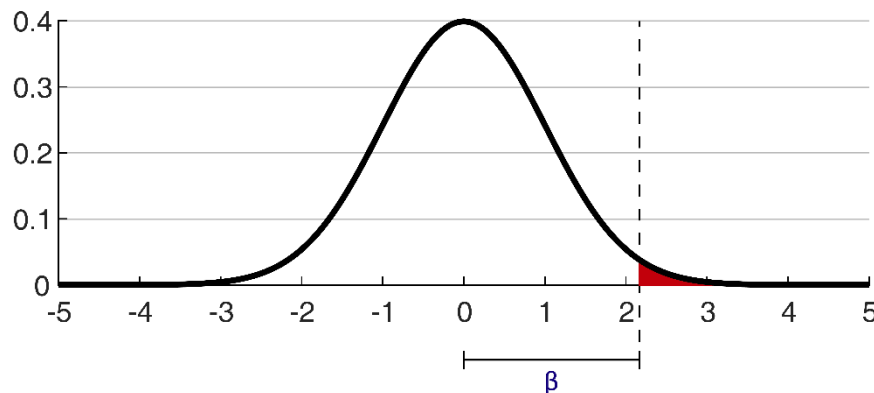
Failure Probability P_f is computed as

$$\beta(t_i, u_0) = \frac{u_0}{\|\mathbf{a}(t_i)\|}$$

$$P_f(E_f : g(t_i, u_0) \leq 0) = \int_{-\infty}^{-\beta} \frac{1}{\sqrt{2\pi}} \exp(-0.5x^2) dx$$

$$= \Phi[-\beta(t_i, u_0)]$$

Probability density function

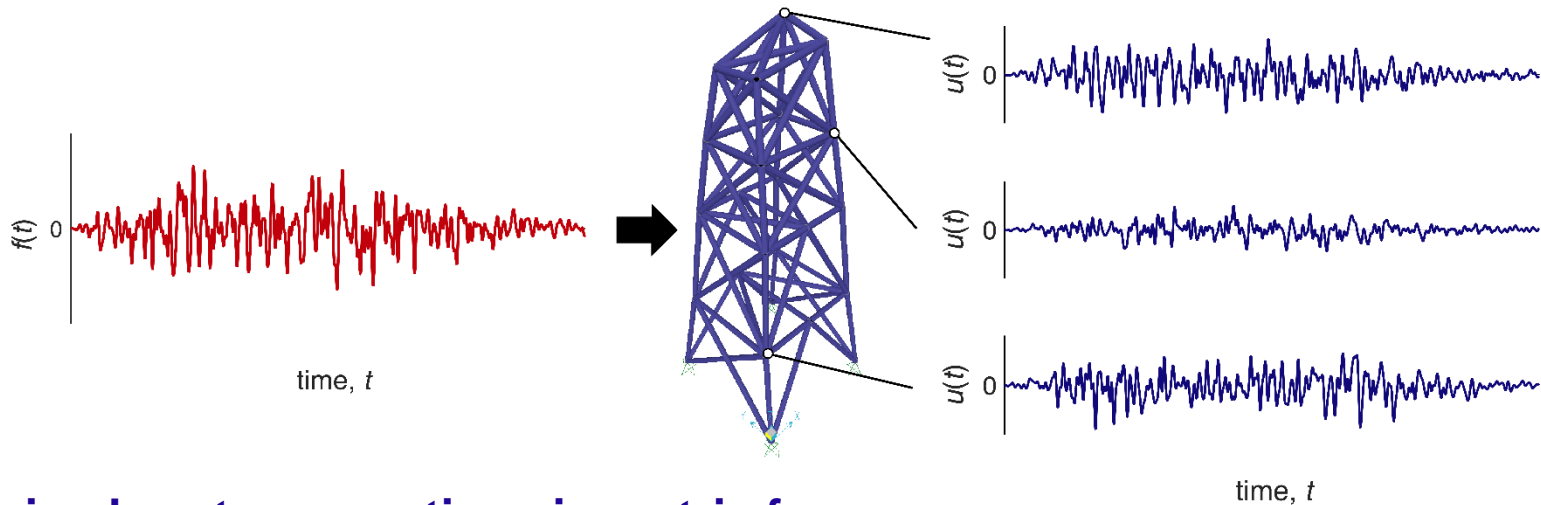


A new procedure to facilitate identifying $a(t)$ without derivation of the impulse response function

□ Numerical Integration (i.e. Newmark method)

$$\dot{u}(t_{j+1}) = \dot{u}(t_j) + [(1-\gamma)\Delta t]\ddot{u}(t_j) + (\gamma\Delta t)\ddot{u}(t_{j+1})$$

$$u(t_{j+1}) = u(t_j) + \Delta t\dot{u}(t_j) + [(0.5-\eta)\Delta t^2]\ddot{u}(t_j) + [\eta\Delta t^2]\ddot{u}(t_{j+1})$$



□ Derived system equations in matrix form

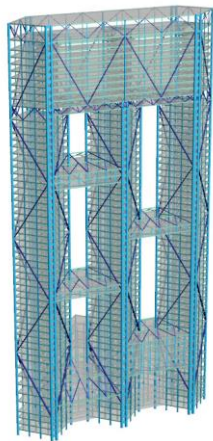
$$\begin{pmatrix} u(t_1) \\ u(t_2) \\ \vdots \\ u(t_{n-1}) \\ u(t_n) \end{pmatrix} = \begin{pmatrix} u(\Delta t) \\ u(2\Delta t) \\ \vdots \\ u(t_0 - \Delta t) \\ u(t_0) \end{pmatrix} = \begin{bmatrix} 0 & 0 & \cdots & 0 & v_1 \\ 0 & 0 & \cdots & v_1 & v_2 \\ \vdots & \vdots & \ddots & \vdots & \vdots \\ 0 & v_1 & \cdots & v_{n-2} & v_{n-1} \\ v_1 & v_2 & \cdots & v_{n-1} & v_n \end{bmatrix} \begin{pmatrix} a_1(t_0) \\ a_2(t_0) \\ \vdots \\ a_{n-1}(t_0) \\ a_n(t_0) \end{pmatrix} \rightarrow a(t_0)$$

Probability of the occurrence of at least one failure event over a time interval needs to be evaluated

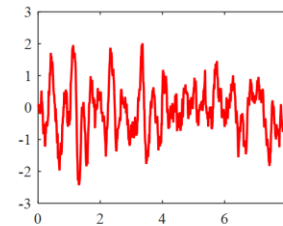
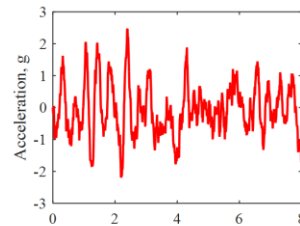
□ Randomness in Dynamic Responses



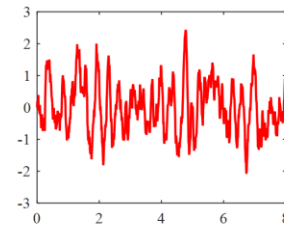
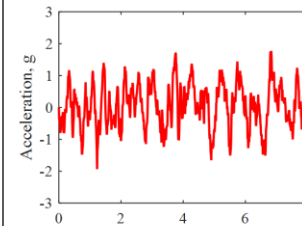
Ssiger International Plaza
Courtesy of Skidmore, Owing and Merrill, LLP



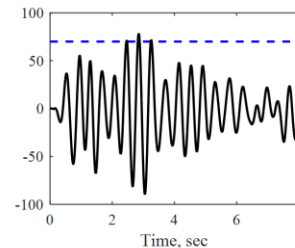
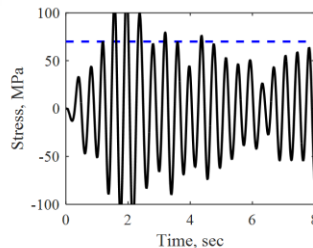
Acceleration



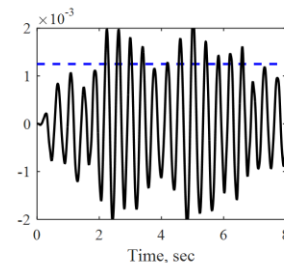
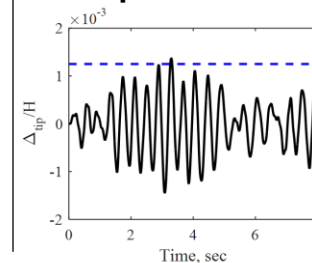
Acceleration



Stress



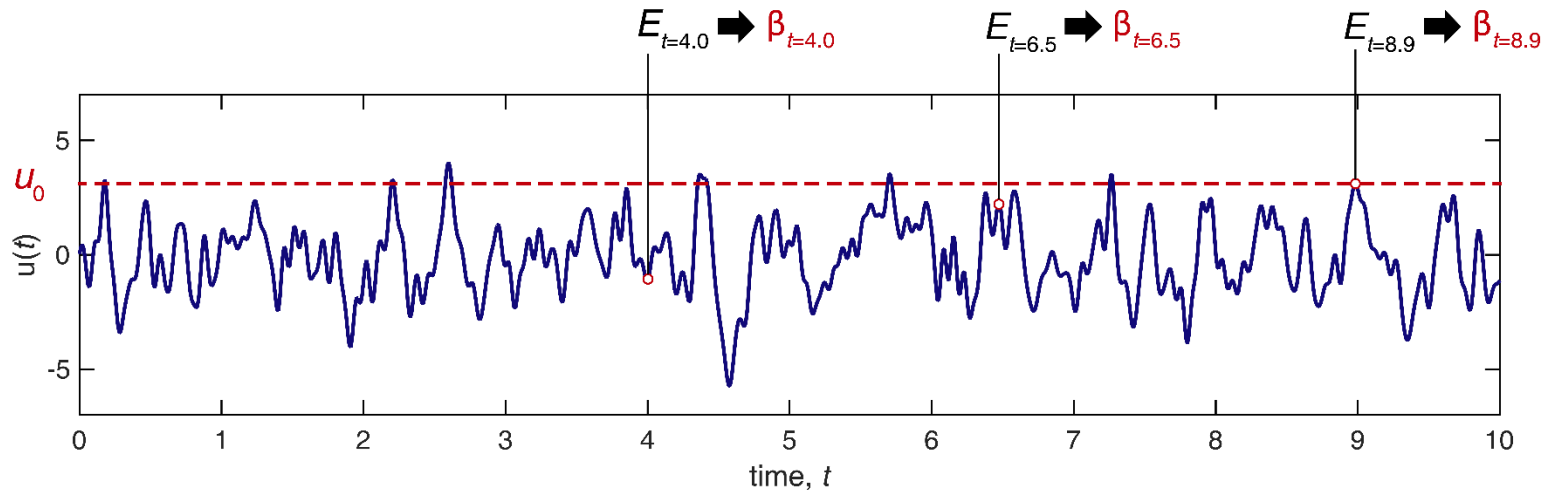
Displacement



In the reliability analysis of **dynamic system** subjected to **stochastic excitations**, a significant problem is determining the **first passage probability** that **any one of output states** of interest **exceeds** a certain threshold value within a given time duration T .

First passage probability is formulated as a series system problem

□ First Passage Probability P_{fp}



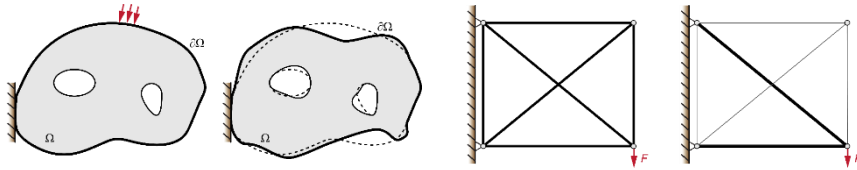
$$P_{fp}(E_{sys}) = P(u_0 < \max_{0 < t < t_n} |u(t)|) = P\left(\bigcup_{i=1}^n |u(t_i)| > u_0\right) = P\left(\bigcup_{i=1}^n E_i\right)$$

$$P_{fp} = \int_{\Omega} \frac{1}{(2\pi)^{n/2} \sqrt{\det \mathbf{R}}} \exp\left(-\frac{1}{2} \mathbf{z}^T \mathbf{R} \mathbf{z}\right) d\mathbf{z} \quad \Omega = \{(z_1, z_2, \dots, z_n) \mid [(z_1 \leq -\beta_1) \cup \dots \cup (z_n \leq -\beta_n)]\}$$

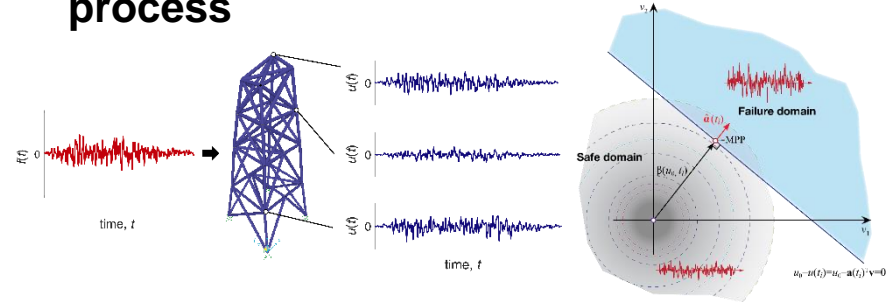
- Main issue:** 1) **Evaluation** of first passage probability in an efficient way
 2) **Sensitivity analysis** for the gradient-based optimization algorithms

Presentation outline

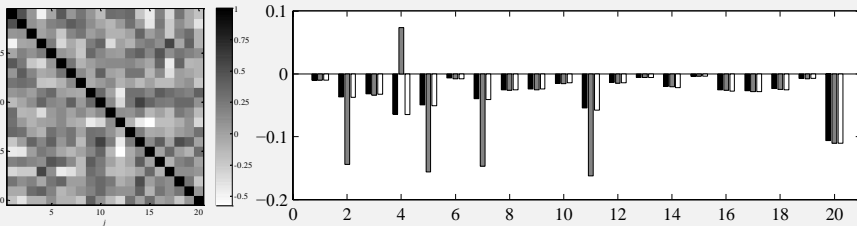
1. Introduction



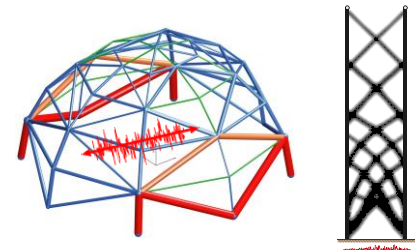
2. Discrete representation of stochastic process



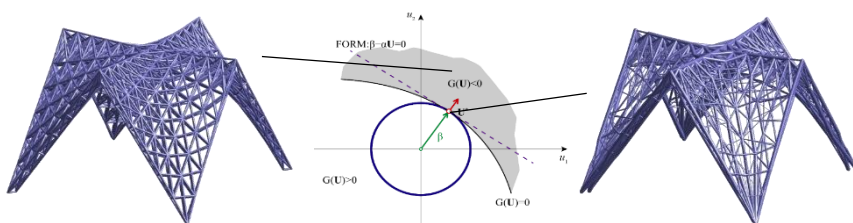
3. Parameter sensitivity of system reliability



4. Structural design and topology optimization under stochastic excitations

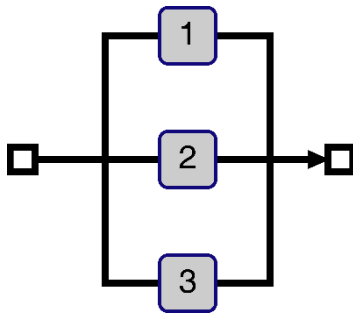
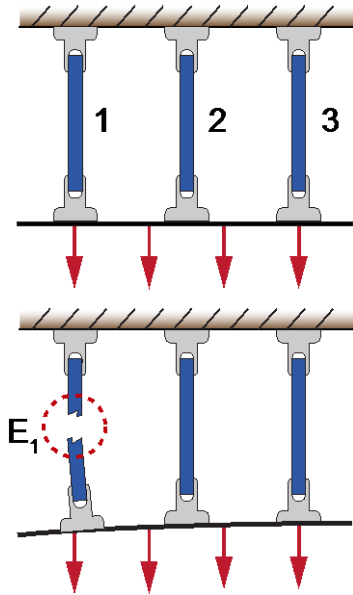


5. Reliability-based topology optimization by ground structure method



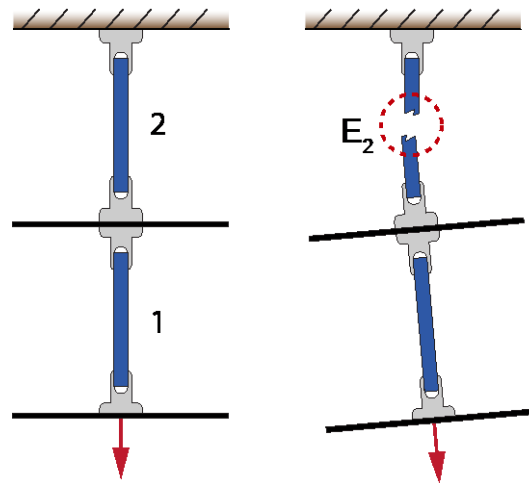
Reliability assessment needs to work with systems having components in parallel, series, and general

□ Parallel System



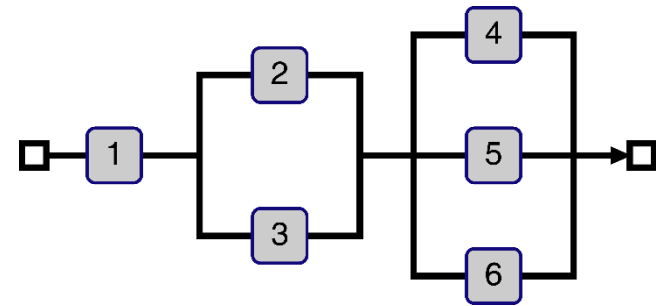
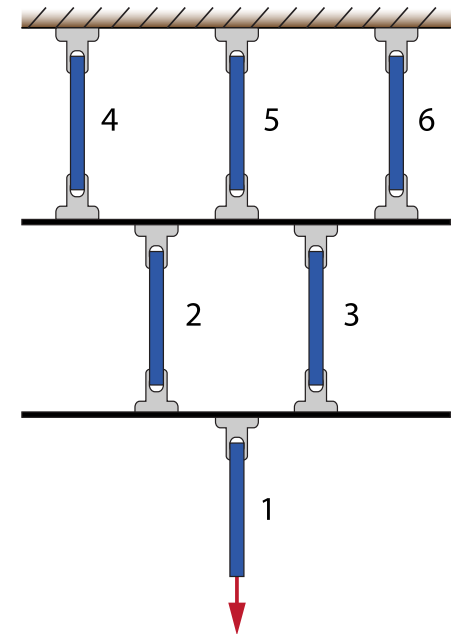
$$E_{parallel} = E_1 \cap E_2 \cap E_3$$

□ Series System



$$E_{series} = E_1 \cup E_2$$

□ General System

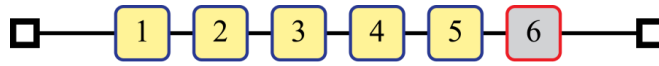


$$E_{general} = E_1 \cup E_2 E_3 \cup E_4 E_5 E_6$$

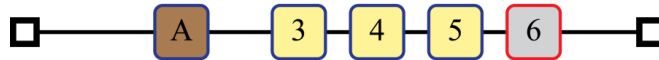
Sequential compounding method (SCM) is an efficient system reliability method

SCM compounds component events coupled by union or intersection sequentially until **a single** compound event **represents** all of the system events

$$P(E_{sys}) = P(E_1 \cup E_2 \cup \dots \cup E_6) = \iiint \iiint \iiint \varphi(\cdot) dz$$



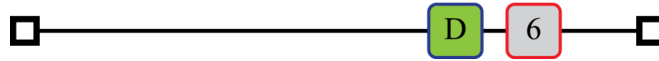
$$P(E_{sys}) = P(E_A \cup E_3 \cup \dots \cup E_6)$$



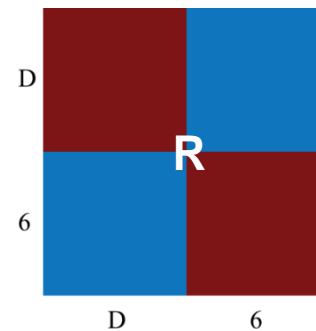
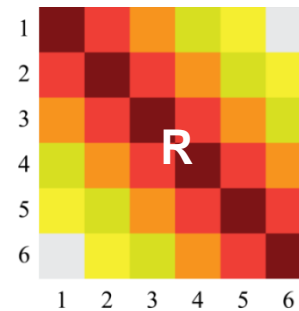
$$P(E_{sys}) = P(E_B \cup E_4 \cup E_5 \cup E_6)$$



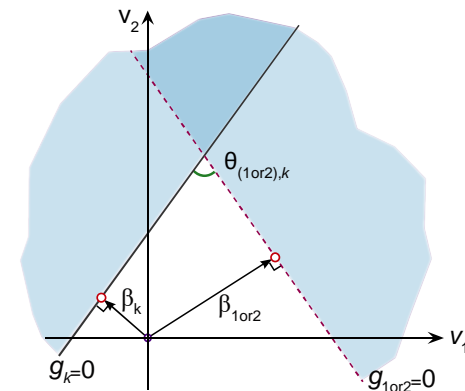
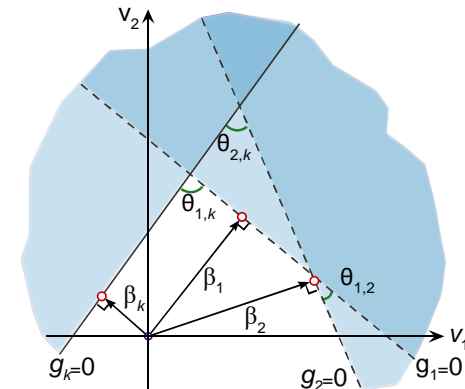
$$P(E_{sys}) = P(E_D \cup E_6)$$



SCM procedure



Correlation matrix



CSP is an efficient sensitivity method for various system problems using SCM

□ Sensitivity in Parallel System

$$P(E_{parallel}) = P(E_k \cap E_{P_k}) = \Phi_2(-\beta_k, -\beta_{P_k}; \rho_{k,P_k})$$

$$\frac{\partial P(E_{parallel})}{\partial \beta_k} = -\varphi(-\beta_k) \cdot \Phi \left[\frac{-\beta_{P_k} + \beta_k \rho_{k,P_k}}{\sqrt{1 - \rho_{k,P_k}^2}} \right]$$

□ Sensitivity in Series System

$$P(E_{series}) = P(E_k \cup E_{S_k})$$

$$\frac{\partial P(E_{series})}{\partial \beta_k} = -\varphi(-\beta_k) \left\{ 1 - \Phi \left[\frac{-\beta_{S_k} + \beta_k \rho_{k,S_k}}{\sqrt{1 - \rho_{k,S_k}^2}} \right] \right\}$$

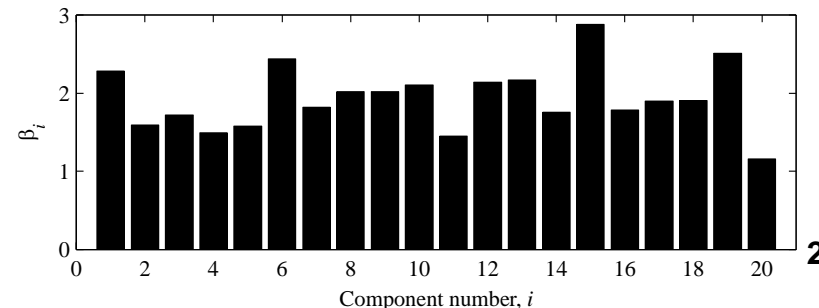
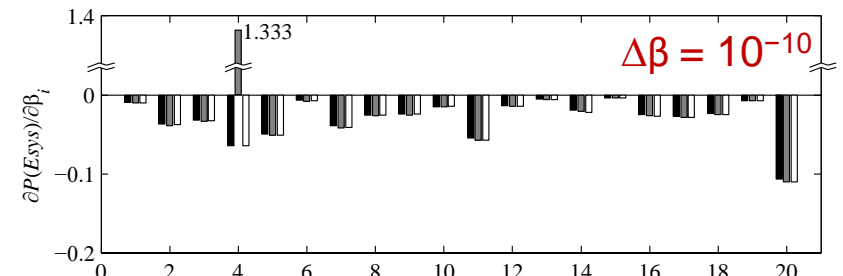
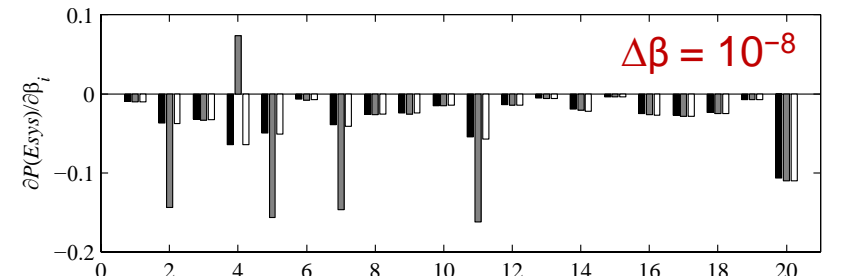
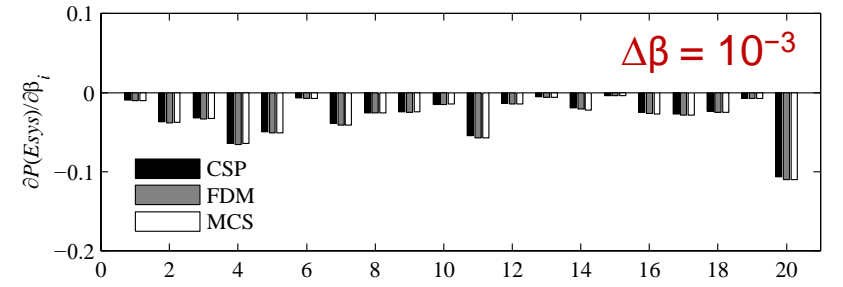
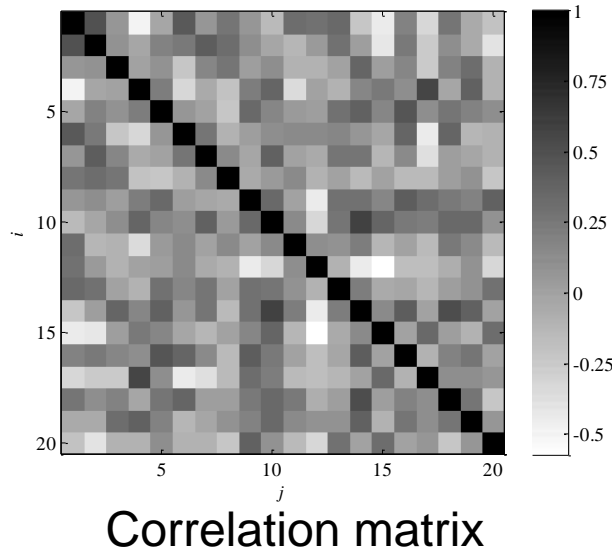
□ Sensitivity in General System

$$P(E_{cut-set}) = P\left(\bigcup_{m=1}^n E_{C_m}\right) = P\left[\bigcup_{m=1}^n \left(\bigcap_{j \in C_m} E_j\right)\right]$$

$$\frac{\partial P(E_{cut-set})}{\partial \beta_k} = \frac{\partial P(E_{cut-set})}{\partial P(E_{C_l})} \cdot \frac{\partial P(E_{C_l})}{\partial \beta_k} = \frac{1}{\varphi(-\beta_{C_l})} \cdot \frac{\partial P(E_{cut-set})}{\partial \beta_{C_l}} \cdot \frac{\partial P(E_{C_l})}{\partial \beta_k}$$

CSP method is tested for a series system consisting of 20 components

Sensitivity calculations by **FDM** may result in **large error** or even different signs depending on perturbation values

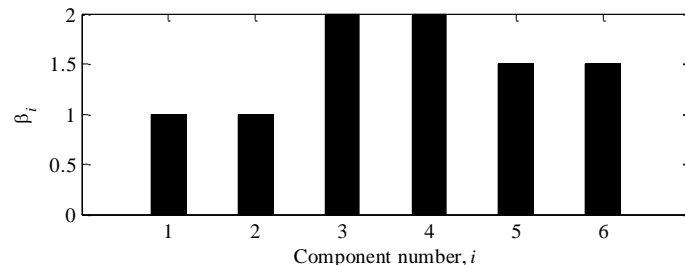
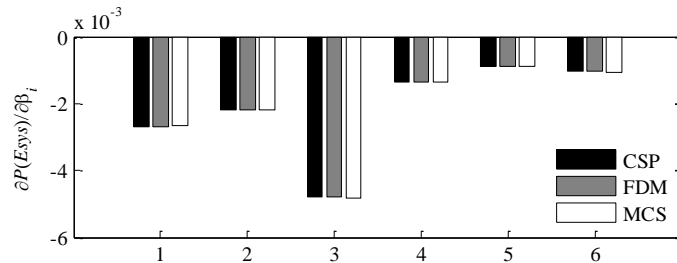
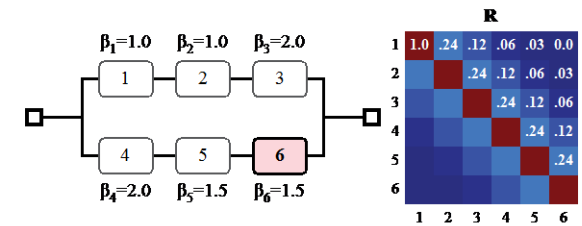
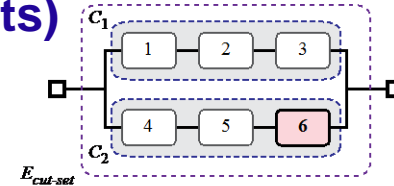


Illustrative example of the CSP method considers the cut-set system problem

General System (two cut-sets and six components)

$$P(E_{sys}) = P(E_{C_1} \cup E_{C_2}) = P(E_1 E_2 E_3 \cup E_4 E_5 E_6)$$

$$\begin{aligned} \frac{\partial P(E_{sys})}{\partial \beta_6} &= -\frac{1}{\varphi(-\beta_{C_2})} \cdot \frac{\partial P(E_{sys})}{\partial \beta_{C_2}} \cdot \frac{\partial P(E_{C_2})}{\partial \beta_6} \\ &= -\frac{1}{0.002423} (0.002398 \times 0.001037) \\ &= -0.001026 \end{aligned}$$



Sensitivities computed by the CSP method, FDM and MCS

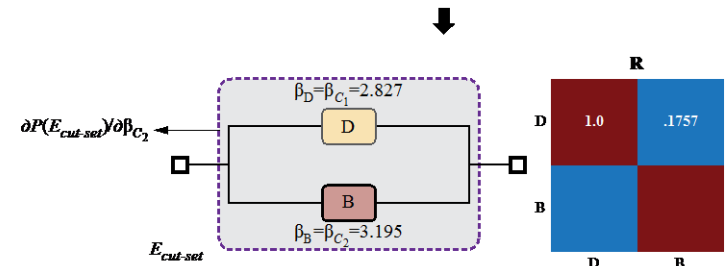
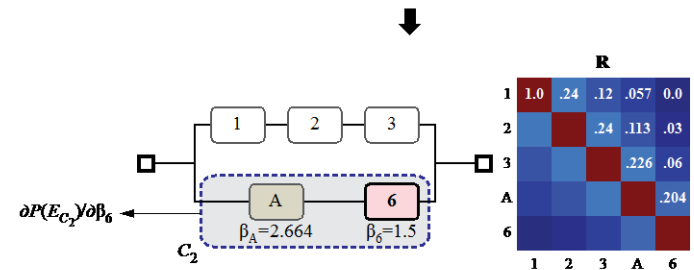


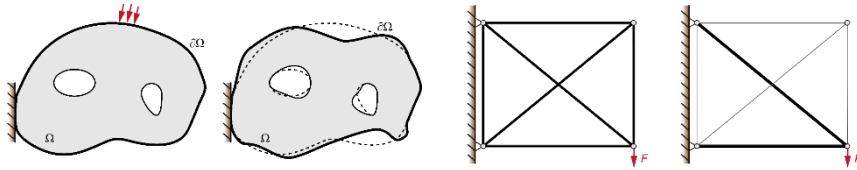
Illustration of the CSP method to compute sensitivity

CSP method remarks

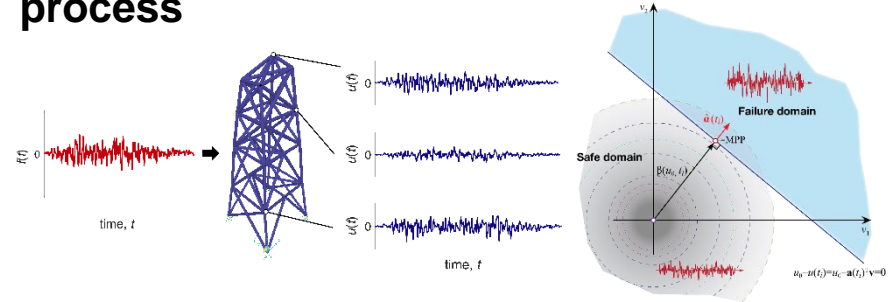
- ❑ CSP method can be used to facilitate efficient use of gradient-based optimization algorithms for design or topology optimization under constraints on system failure probability
- ❑ New sensitivity method, **CSP**, was developed to compute the parameter sensitivity of series, parallel and general system problems using **SCM**
- ❑ Sequential Compounding Method (**SCM**) was reviewed
- ❑ Sensitivity computed by CSP, FDM, and MCS were compared with respect to accuracy

Presentation outline

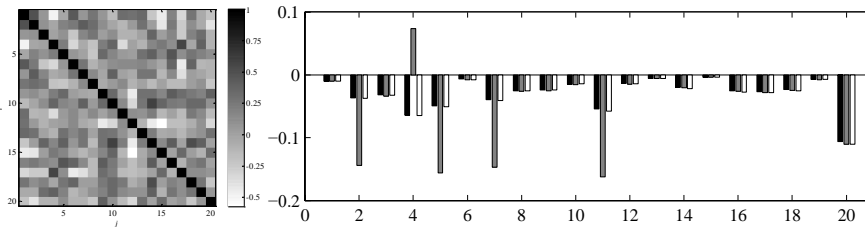
1. Introduction



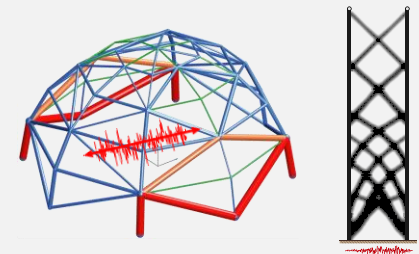
2. Discrete representation of stochastic process



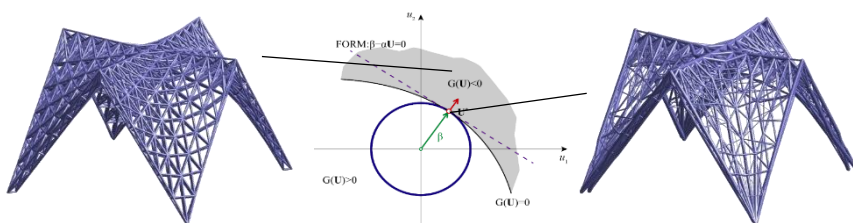
3. Parameter sensitivity of system reliability



4. Structural design and topology optimization under stochastic excitations



5. Reliability-based topology optimization by ground structure method



RBDO & RBTO aims to achieve the optimal design under probabilistic constraints on uncertain performance

□ System Reliability Based Design Optimization (SRBDO) problem

$$\begin{aligned} \min_{\mathbf{d}} \quad & f_{obj}(\mathbf{d}) \\ \text{s.t.} \quad & P(E_{sys}^i) = P\left(\bigcup_{k=1}^n E_{f_i}(t_k, \mathbf{d})\right) = P\left(\bigcup_{k=1}^n \{g_i(t_k, \mathbf{d}) \leq 0\}\right) \leq P_{f_i}^{target}, \quad i = 1, \dots, n_c \\ & \mathbf{d}^{lower} \leq \mathbf{d} \leq \mathbf{d}^{upper} \\ \text{with} \quad & \mathbf{M}(\mathbf{d})\ddot{\mathbf{u}}(t, \mathbf{d}) + \mathbf{C}(\mathbf{d})\dot{\mathbf{u}}(t, \mathbf{d}) + \mathbf{K}(\mathbf{d})\mathbf{u}(t, \mathbf{d}) = \mathbf{f}(t, \mathbf{d}) \end{aligned}$$

□ Rayleigh Damping Model

$$\mathbf{C} = \kappa_0 \mathbf{M} + \kappa_1 \mathbf{K}$$

□ Earthquake Ground Excitation

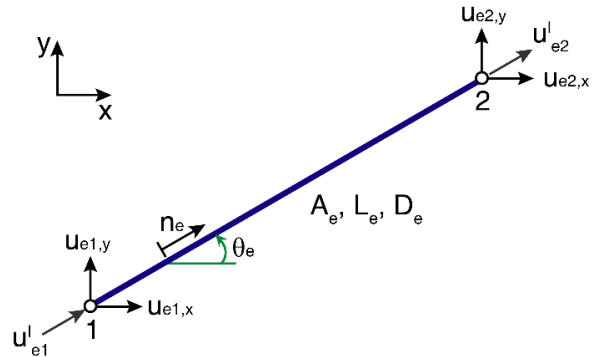
$$\mathbf{f}(t, \mathbf{d}) = -\mathbf{M}(\mathbf{d})\ddot{u}_g(t) = -\mathbf{M}(\mathbf{d})\mathbf{l}f(t) = -\mathbf{M}(\mathbf{d})\mathbf{l} \cdot \left(\int_0^t h_f^{KT}(t-\tau)W(\tau)d\tau \right)$$

□ Kanai-Tajimi filter

$$h_f^{KT}(t) = \exp(-\zeta_f \omega_f t) \left[\frac{(2\zeta_f^2 - 1)\omega_f}{\sqrt{1 - \zeta_f^2}} \sin(\omega_f \sqrt{1 - \zeta_f^2} \cdot t) - 2\zeta_f \omega_f \cos(\omega_f \sqrt{1 - \zeta_f^2} \cdot t) \right]$$

Various engineering constraints can be incorporated into RBDO&RBTO under first passage probability

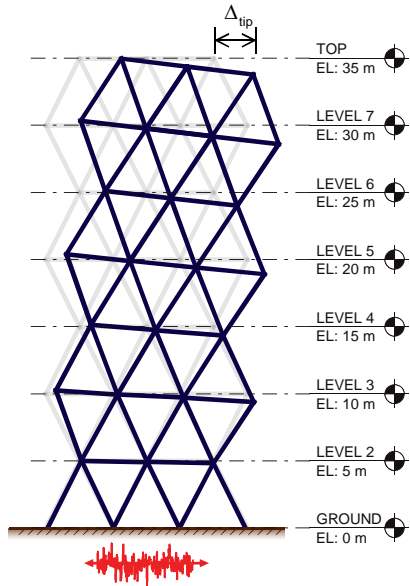
□ Stress in Bar



$$\begin{aligned}\sigma_e(t, \mathbf{d}) &= \frac{D_e}{L_e} \mathbf{n}_e \cdot (\mathbf{u}_{e2}^g(t, \mathbf{d}) - \mathbf{u}_{e1}^g(t, \mathbf{d})) \\ &= \frac{D_e}{L_e} (u_{e2}^l(t, \mathbf{d}) - u_{e1}^l(t, \mathbf{d}))\end{aligned}$$

$$E_{fe}(t_k, \mathbf{d}) : \sigma_{oe} - \sigma_e(t_k, \mathbf{d}) \leq 0$$

□ Maximum Displacement

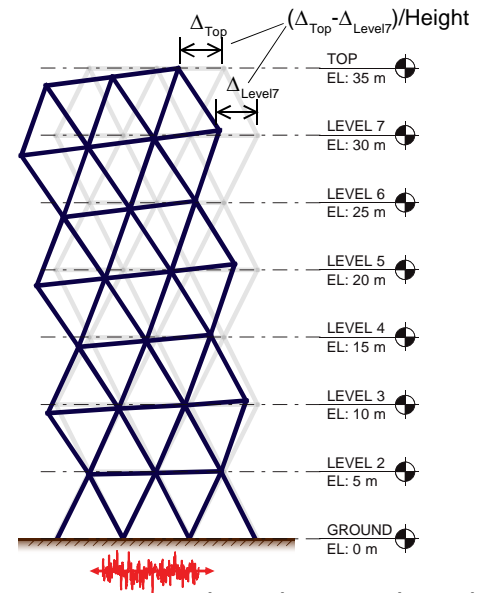


$$E_{f_\Delta}(t_k, \mathbf{d}) : u_{o\Delta} - \Delta_{tip}(t_k, \mathbf{d}) \leq 0$$



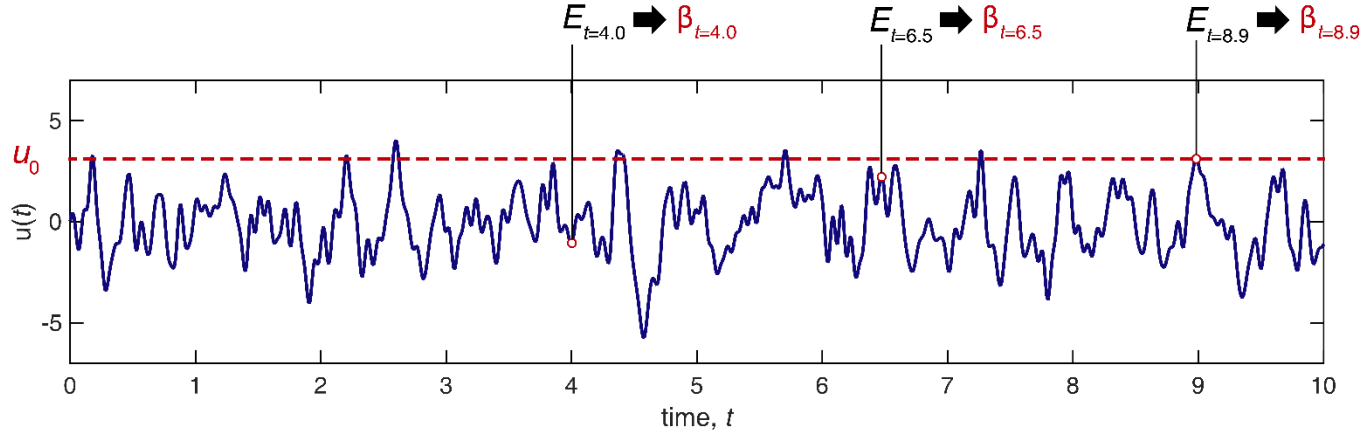
Hearst Tower (New York City)
<http://www.sefindia.org/>

□ Inter-story Drift Ratio



$$E_{f_{\Delta_i}}(t_k, \mathbf{d}) : u_{o\Delta_i} - \frac{\Delta_i(t_k, \mathbf{d}) - \Delta_{i-1}(t_k, \mathbf{d})}{H_i} \leq 0$$

Computation of first passage probability of engineering constraint



$$\begin{aligned}
 P_{fp}(E_{sys}) &= P_{fp}\left(\bigcup_{k=1}^n E_{f_i}(t_k, \mathbf{d})\right) \\
 &= 1 - \Phi_n\left[\beta_i(t_1, \mathbf{d}), \beta_i(t_2, \mathbf{d}), \dots, \beta_i(t_{nt}, \mathbf{d}); \rho_{1,2}, \rho_{1,3}, \dots, \rho_{n-1,n}\right] \\
 &= 1 - \Phi_n[\boldsymbol{\beta}_i, \mathbf{R}]
 \end{aligned}
 \quad \mathbf{R} = \begin{bmatrix} \rho_{1,1} & \cdots & \rho_{1,n} \\ \vdots & \ddots & \vdots \\ \rho_{n,1} & \cdots & \rho_{n,n} \end{bmatrix}$$

Parameter sensitivity of first passage probability in RBDO&RBTO

$$\begin{aligned}
 \frac{\partial P_{fp}(E_{sys})}{\partial d_i} &= \frac{\partial(1 - \Phi_n[\boldsymbol{\beta}_i, \mathbf{R}])}{\partial d_i} = \sum_{j=1}^n \left(\frac{\partial(-\Phi_n[\boldsymbol{\beta}_i, \mathbf{R}])}{\partial \beta_j} \cdot \frac{\partial \beta_j(\mathbf{d})}{\partial d_i} \right) = \sum_{j=1}^n \left(c_j \cdot \frac{\partial \beta_j(\mathbf{d})}{\partial d_i} \right) \\
 \frac{\partial \beta_j(\mathbf{d})}{\partial d_i} &= - \frac{C_{cst} \cdot \left(\sum_{k=1}^j \left(a_k(t_j, \mathbf{d}) \cdot \frac{\partial a_k(t_j, \mathbf{d})}{\partial d_i} \right) \right)}{\left(\sum_{k=1}^j a_k(t_j, \mathbf{d})^2 \right)^{3/2}}
 \end{aligned}$$

Implicit derivatives can be eliminated through adjoint method

□ Adjoint Method (AJM)

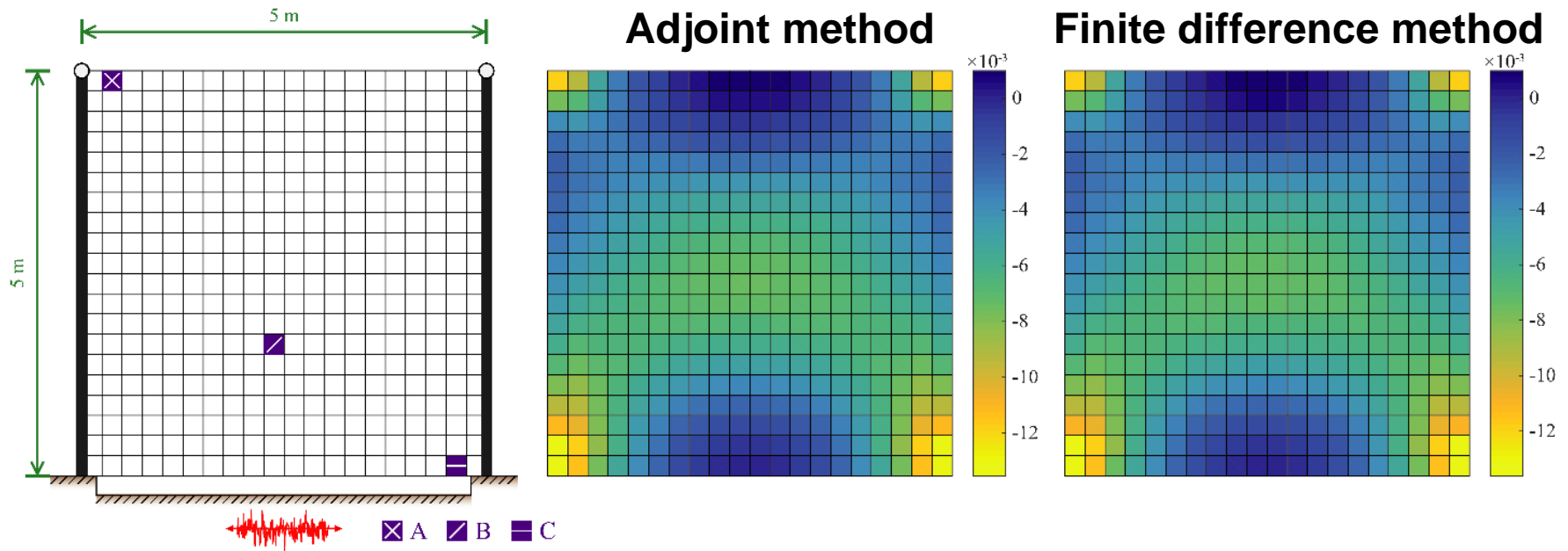
AJM introduces an adjoint system of equations so that computation of implicitly defined terms can be avoided. This results in significant reduction of computational cost.

$$\frac{\partial P_{fp}(E_{sys})}{\partial d_i} = \sum_{j=1}^n \left(c_j \cdot \frac{\partial \beta_j(\mathbf{d})}{\partial d_i} \right) + \sum_{j=1}^n \boldsymbol{\lambda}_{n-j+1}^\top \left[\mathbf{M}(\mathbf{d})\ddot{\mathbf{u}}(t_j, \mathbf{d}) + \mathbf{C}(\mathbf{d})\dot{\mathbf{u}}(t_j, \mathbf{d}) + \mathbf{K}(\mathbf{d})\mathbf{u}(t_j, \mathbf{d}) + \mathbf{M}(\mathbf{d})\mathbf{f}(t_j, \mathbf{d}) \right]$$



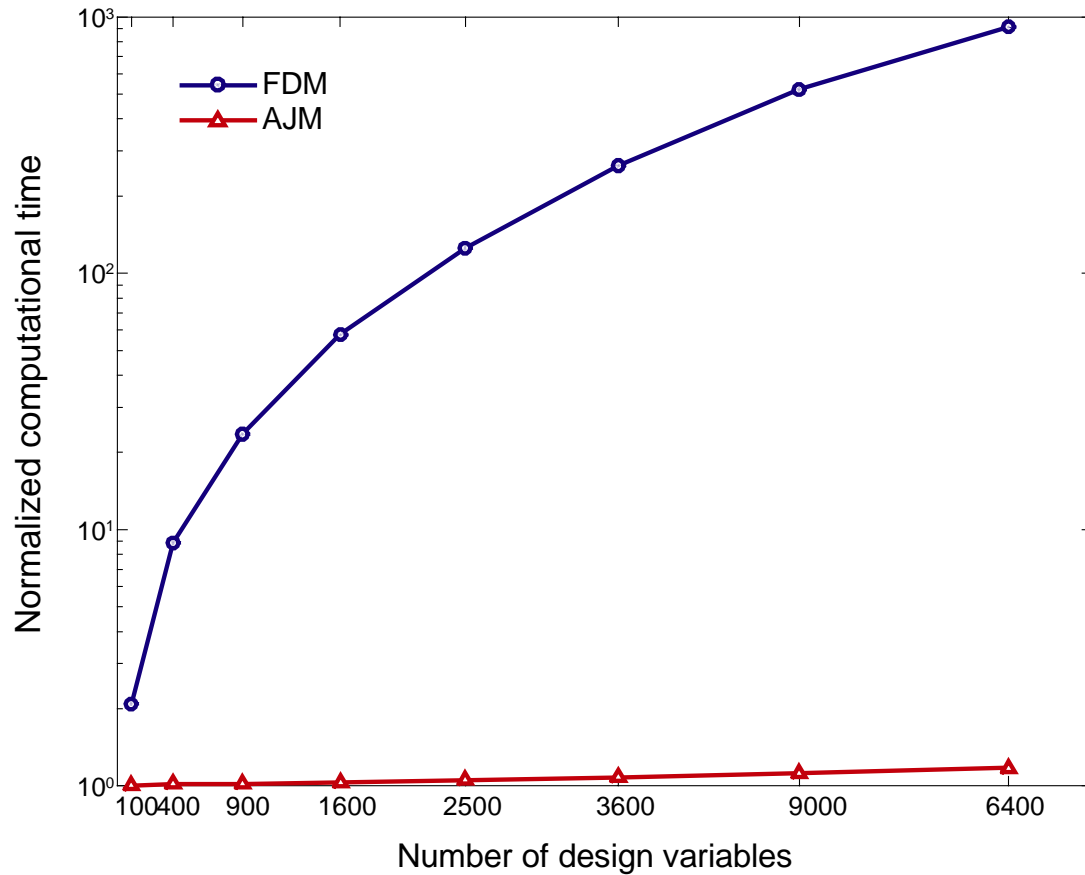
$$\begin{aligned} \frac{\partial P_{fp}(E_{sys})}{\partial d_i} = & \sum_{j=1}^n \boldsymbol{\lambda}_{n-j+1}^\top \left[\frac{\partial \tilde{\mathbf{A}}(\mathbf{d})}{\partial d_i} \cdot \mathbf{u}(t_j, \mathbf{d}) - \eta(\Delta t)^2 \frac{\partial \mathbf{f}(t_j, \mathbf{d})}{\partial d_i} - (0.5 + \gamma - 2\eta)(\Delta t)^2 \frac{\partial \mathbf{f}(t_{j-1}, \mathbf{d})}{\partial d_i} \right. \\ & \left. - (0.5 - \gamma + \eta)(\Delta t)^2 \frac{\partial \mathbf{f}(t_{j-2}, \mathbf{d})}{\partial d_i} + \frac{\partial \mathbf{B}(\mathbf{d})}{\partial d_i} \cdot \mathbf{u}(t_{j-1}, \mathbf{d}) + \frac{\partial \mathbf{E}(\mathbf{d})}{\partial d_i} \cdot \mathbf{u}(t_{j-2}, \mathbf{d}) \right] \\ & + \boldsymbol{\lambda}_n^\top \left[\frac{\partial \mathbf{B}(\mathbf{d})}{\partial d_i} \cdot \mathbf{u}(0, \mathbf{d}) + \frac{\partial \mathbf{E}(\mathbf{d})}{\partial d_i} \cdot \mathbf{u}(t_{-1}, \mathbf{d}) \right] + \boldsymbol{\lambda}_{n-1}^\top \left[\frac{\partial \mathbf{E}(\mathbf{d})}{\partial d_i} \cdot \mathbf{u}(0, \mathbf{d}) \right] \end{aligned}$$

Sensitivities of first passage probability from AJM show a good agreement with those by FDM



| Δd | FDM | | | AJM | | |
|---------------------|-----------------------------|-----------------------------|-----------------------------|-----------------------------|-----------------------------|-----------------------------|
| | $\partial P / \partial d_A$ | $\partial P / \partial d_B$ | $\partial P / \partial d_C$ | $\partial P / \partial d_A$ | $\partial P / \partial d_B$ | $\partial P / \partial d_C$ |
| 1×10^{-1} | -0.000452 | -0.000293 | -0.000569 | | | |
| 1×10^{-2} | -0.000483 | -0.000310 | -0.000596 | | | |
| 1×10^{-3} | -0.000486 | -0.000312 | -0.000599 | | | |
| 1×10^{-4} | -0.000487 | -0.000312 | -0.000599 | | | |
| 1×10^{-5} | -0.000487 | -0.000312 | -0.000599 | | | |
| 1×10^{-6} | -0.000486 | -0.000312 | -0.000599 | | | |
| 1×10^{-7} | -0.000485 | -0.000309 | -0.000598 | -0.000486 | -0.000312 | -0.000599 |
| 1×10^{-8} | -0.000479 | -0.000301 | -0.000619 | | | |
| 1×10^{-9} | -0.000444 | -0.000391 | -0.000632 | | | |
| 1×10^{-10} | 0.000250 | 0.000289 | -0.000012 | | | |
| 1×10^{-11} | -0.000166 | -0.001532 | -0.004141 | | | |
| 1×10^{-12} | 0.050625 | 0.025424 | 0.036526 | | | |

Numerical tests confirm significant reduction in computational time of proposed AJM compared to FDM



Optimization of a lateral bracing system subjected to earthquake ground motions

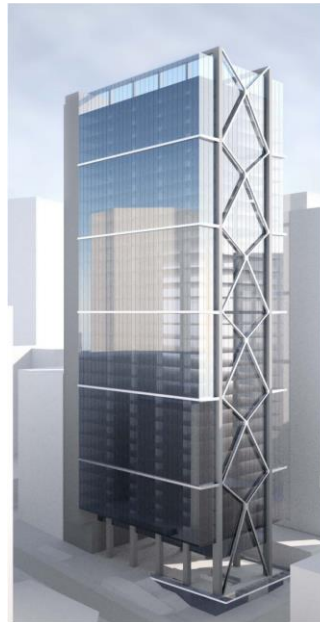
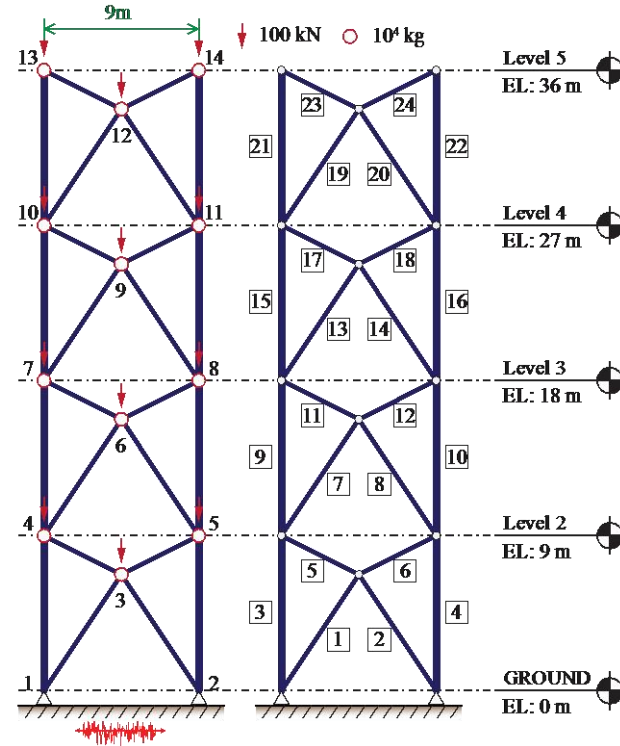


Image courtesy of SOM



$E = 21,000 \text{ MPa}$
 $\rho_m = 2,400 \text{ kg/m}^3$

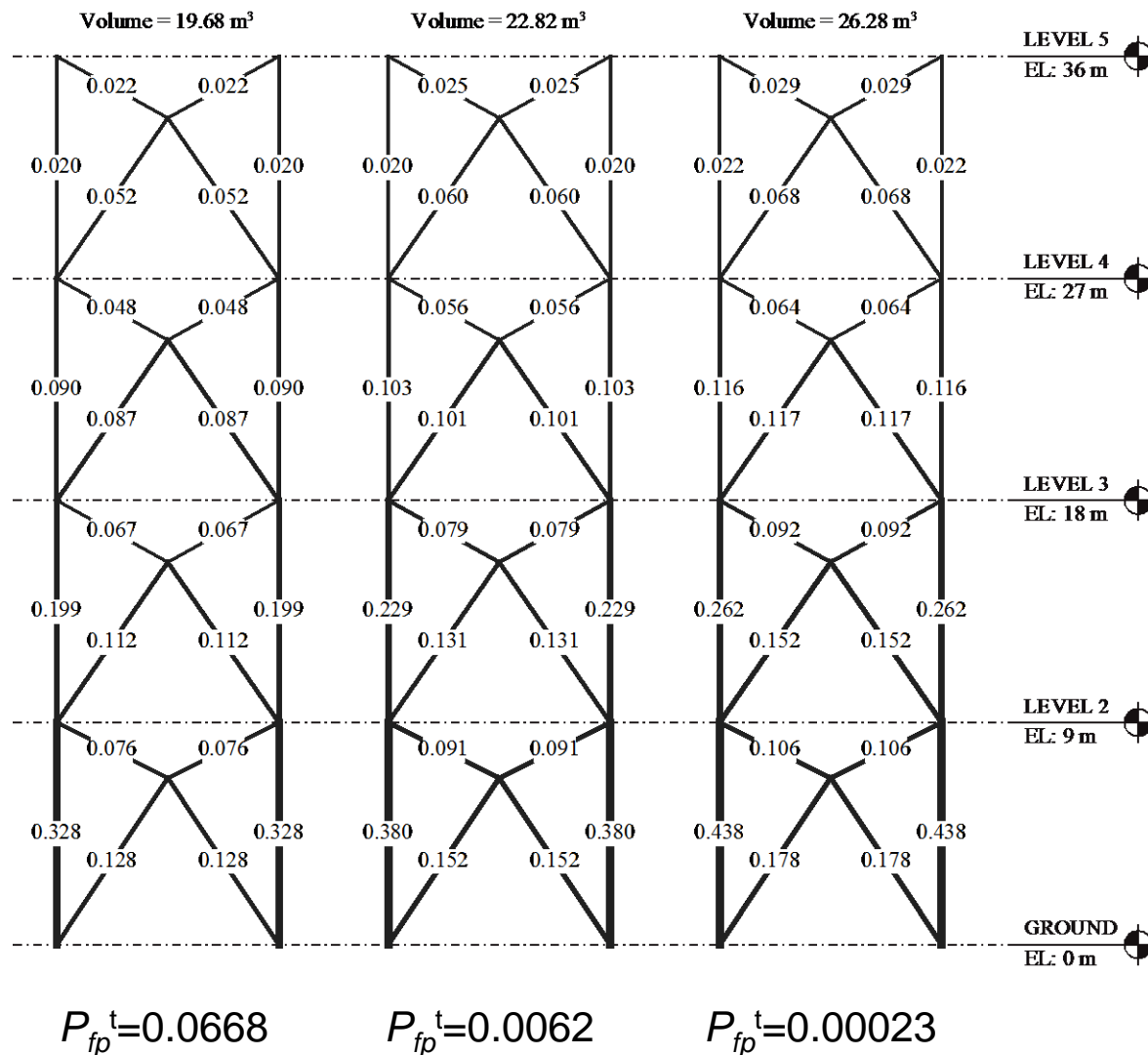
$$\min_{\mathbf{d}} \quad \text{volume}$$

$$\text{s.t.} \quad P_{fp,i}(\text{stress}, \sigma_{oe} = 35 \text{ MPa}) \leq P_f^{\text{target}}, \quad i = 1, \dots, n_c$$

$$0.02 \text{ m}^2 \leq \mathbf{d} \leq 1 \text{ m}^2$$

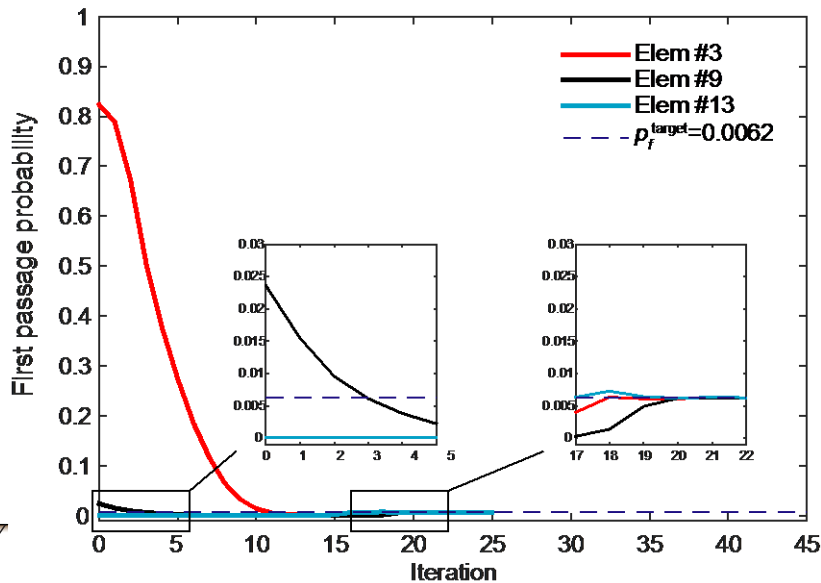
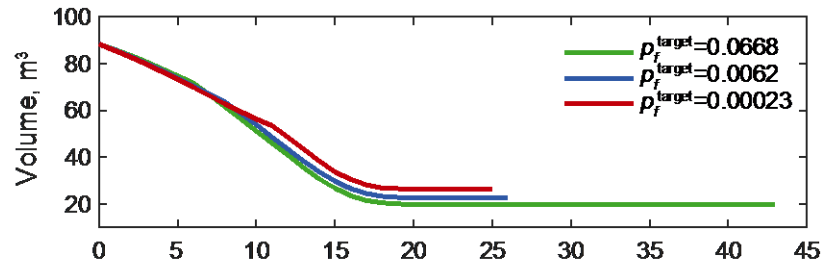
$$\text{with} \quad \mathbf{M}(\mathbf{d})\ddot{\mathbf{u}}(t, \mathbf{d}) + \mathbf{C}(\mathbf{d})\dot{\mathbf{u}}(t, \mathbf{d}) + \mathbf{K}(\mathbf{d})\mathbf{u}(t, \mathbf{d}) = -\mathbf{M}(\mathbf{d})\mathbf{f}(t)$$

Proposed method enables optimization of elements for different target first passage failure probabilities

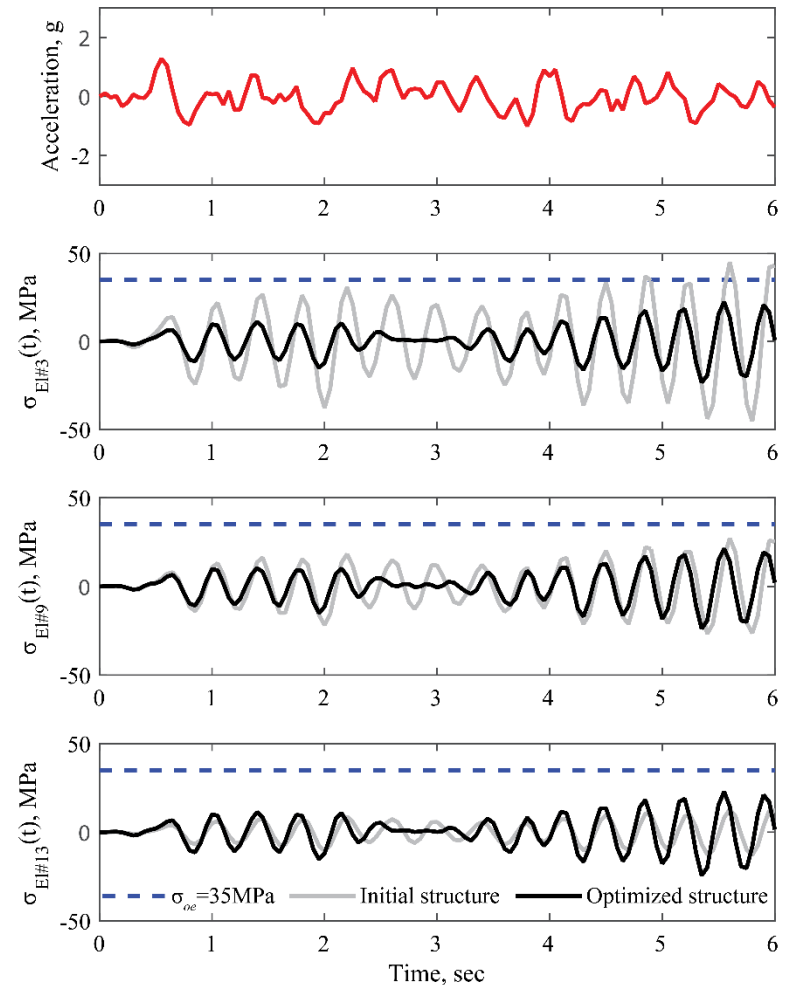


Reduction of stress time histories decreases likelihood of exceeding the threshold value for P_f^{target}

Convergence History

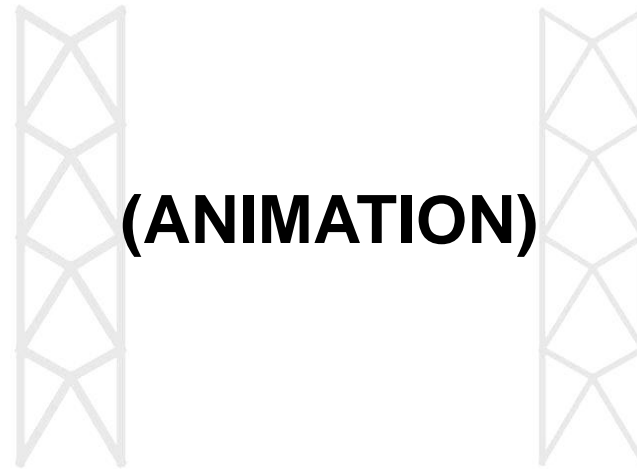
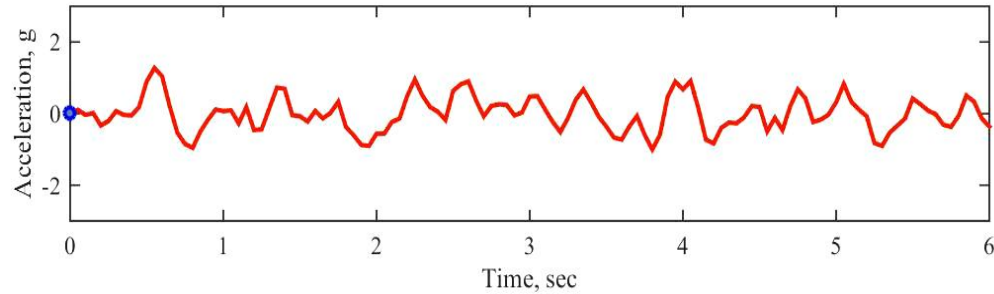


Dynamic Response Comparison



Stress time histories are more uniform than stress levels shown in the initial structure

Dynamic Behavior (Stress)



Initial System

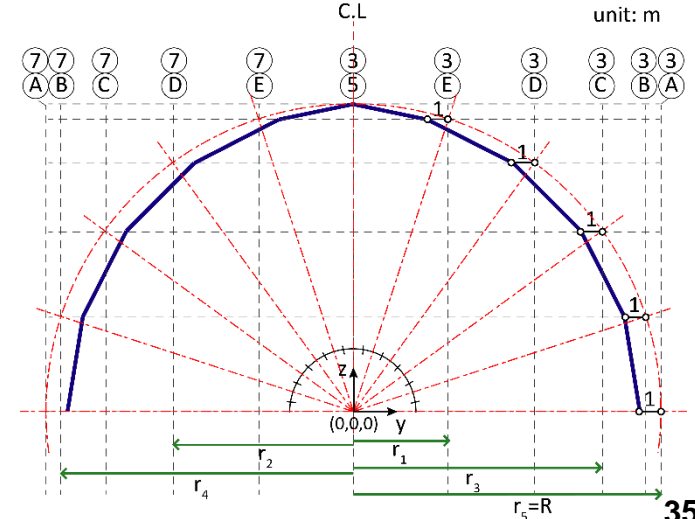
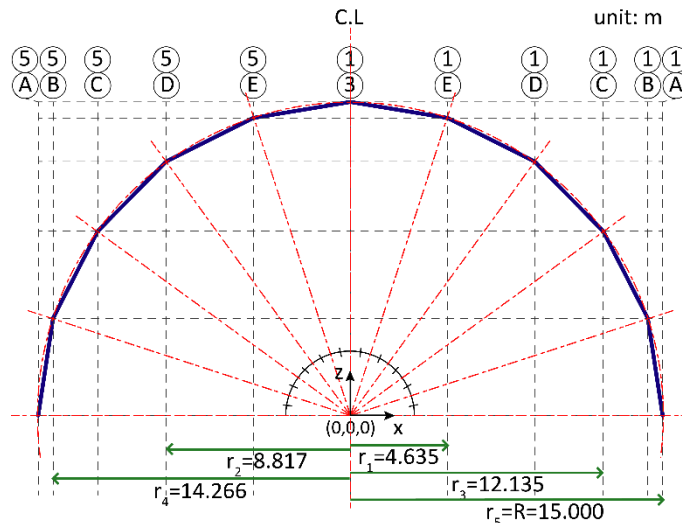
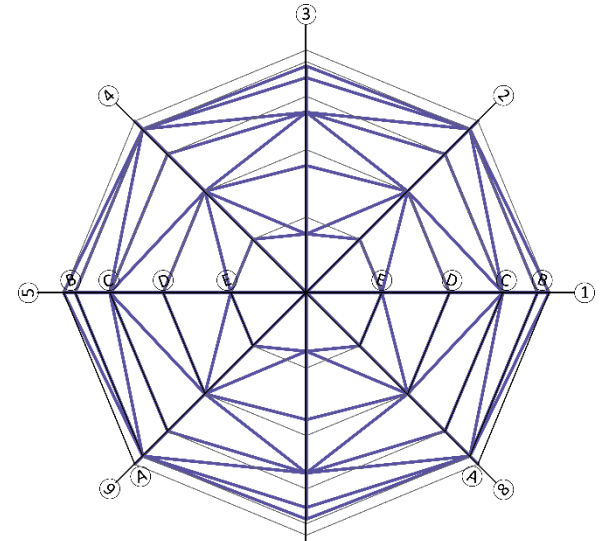
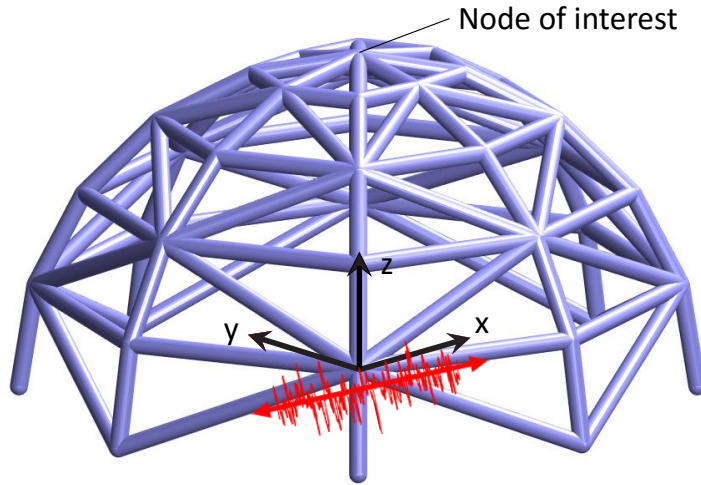
Optimized System



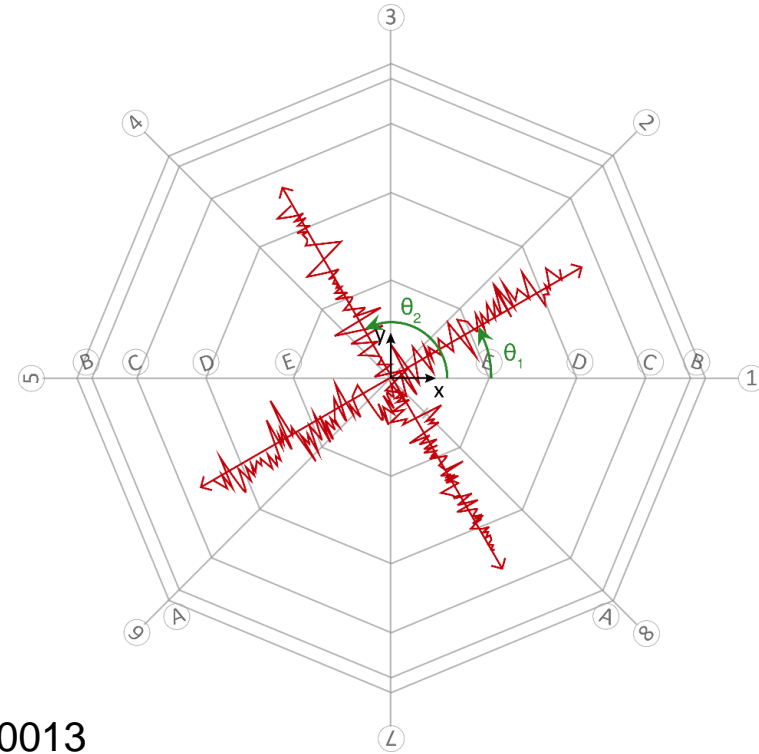
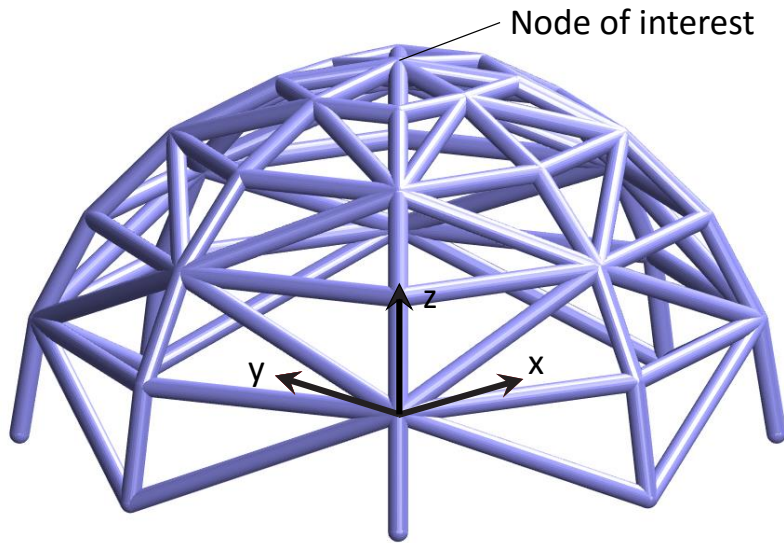
Optimization of space truss dome subjected to stochastic excitations

Space Truss Dome

$E = 210 \text{ GPa}$
 $\rho_m = 7,850 \text{ kg/m}^3$
 2% damping ratio



Simultaneous considerations of two direction components of earthquake ground excitations at different angles



min \mathbf{d} volume

s.t P_{fp} (drift ratio in x-direction) ≤ 0.0013

P_{fp} (drift ratio in y-direction) ≤ 0.0013

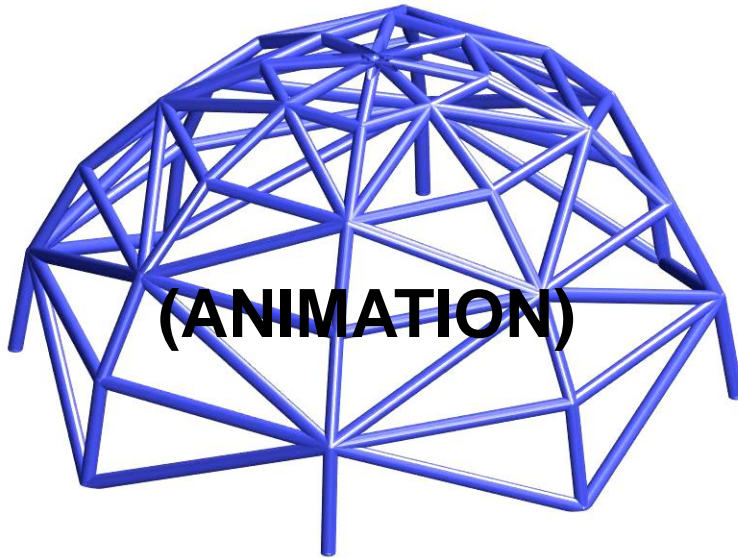
$0.02 \text{ m}^2 \leq \mathbf{d} \leq 1.5 \text{ m}^2$

with $\mathbf{M}(\mathbf{d})\ddot{\mathbf{u}}(t, \mathbf{d}) + \mathbf{C}(\mathbf{d})\dot{\mathbf{u}}(t, \mathbf{d}) + \mathbf{K}(\mathbf{d})\mathbf{u}(t, \mathbf{d}) = -\mathbf{M}(\mathbf{d})\mathbf{l}(\theta_{g1})f_{g1}(t) - \mathbf{M}(\mathbf{d})\mathbf{l}(\theta_{g2})f_{g2}(t)$

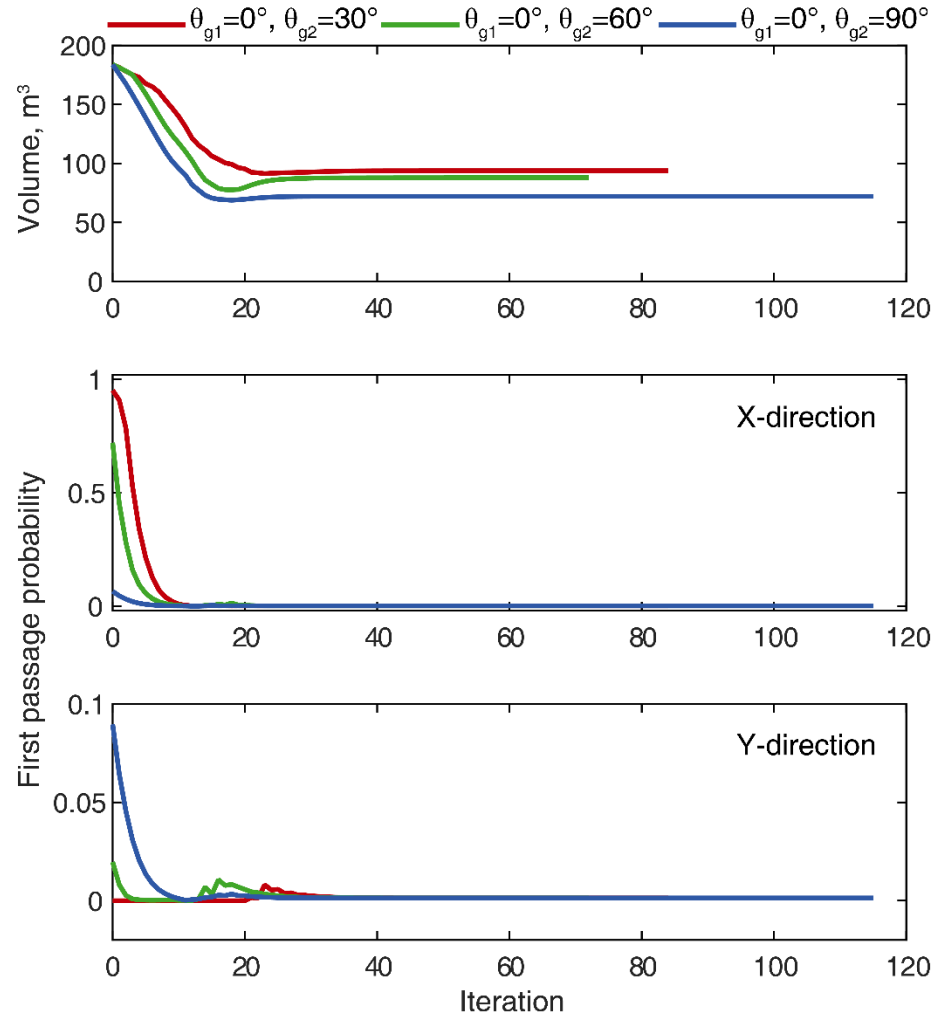
| Φ_{g1o} | Φ_{g2o} | ω_f | ζ_f | t (sec) | Δt (sec) | Initial Area (m ²) | Threshold value |
|--------------|--------------|------------|-----------|-----------|------------------|--------------------------------|--|
| 4.0 | 3.0 | 5π | 0.4 | 6.0 | 0.06 | 0.25 | $u_{o\Delta x} = 1/800$ $u_{o\Delta y} = 1/800$ |

Optimization history: volume reduction while satisfying the target failure probability

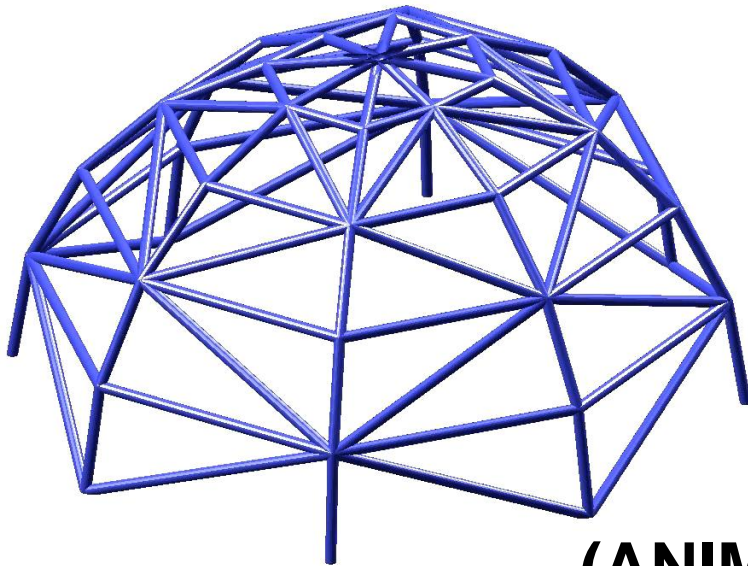
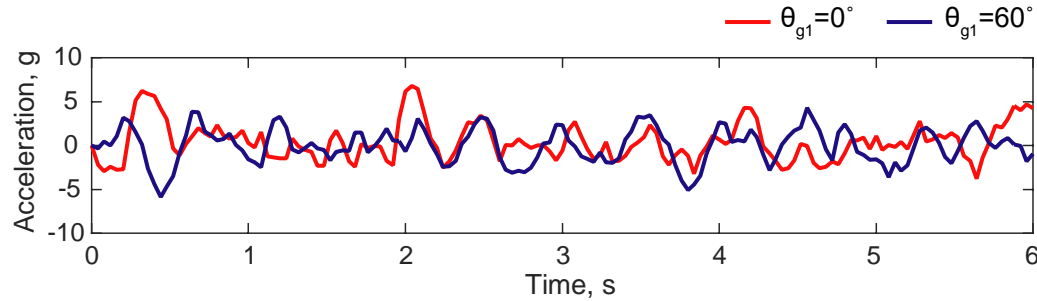
Iter: 1, Volume = 183.85 m³



Convergence History

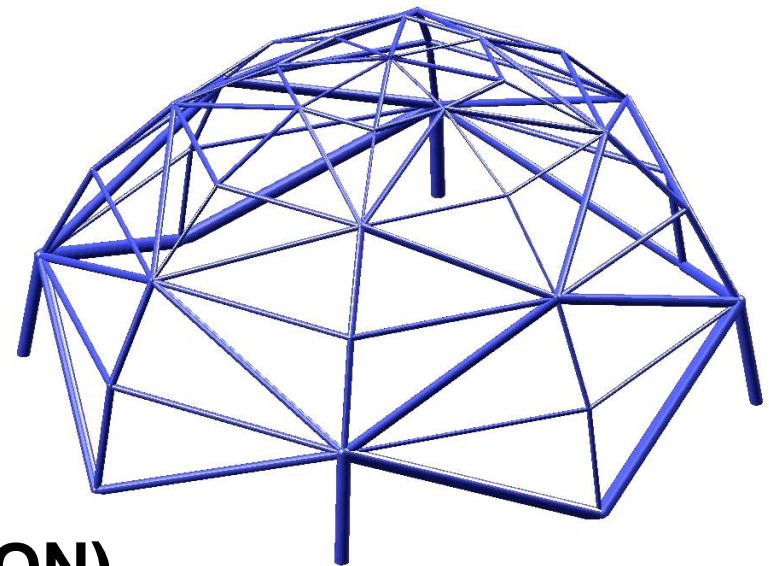


Comparison of dynamic responses of the initial structure and optimized structures



Initial structure

(ANIMATION)

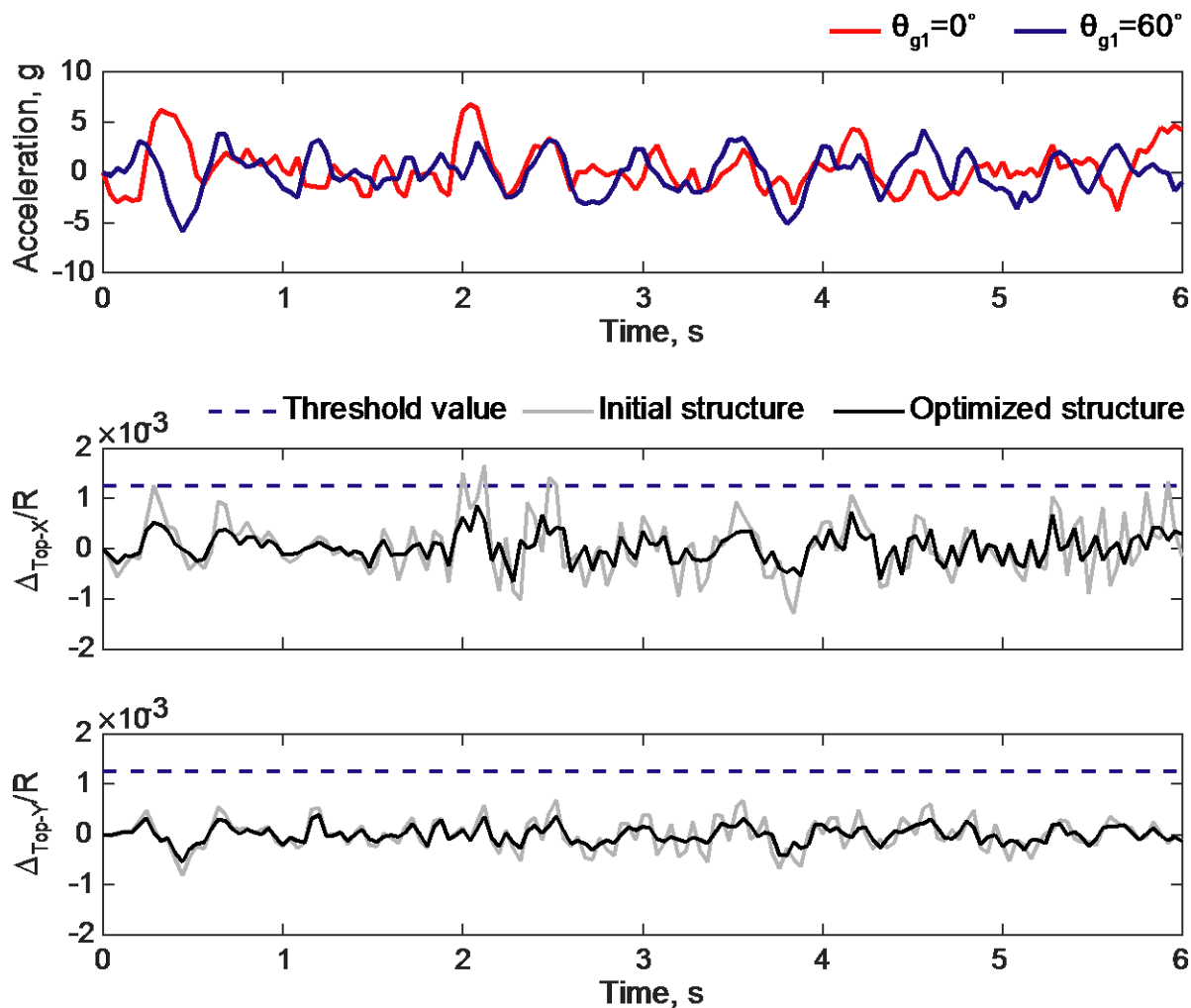


Optimized structure

Scale Factor = 5

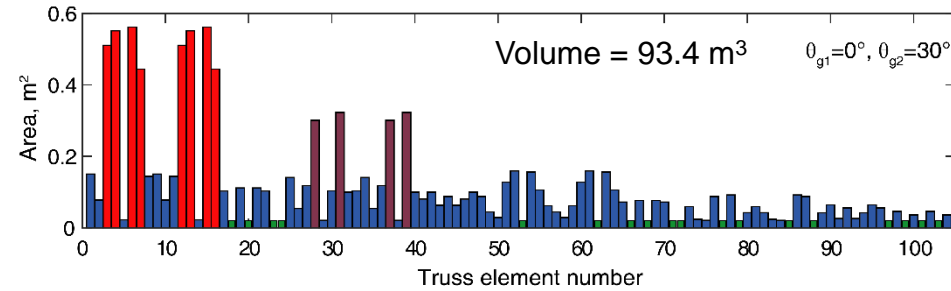
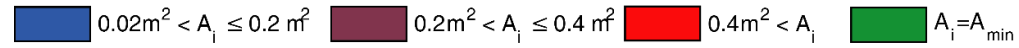
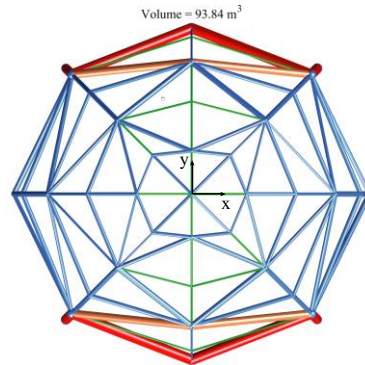
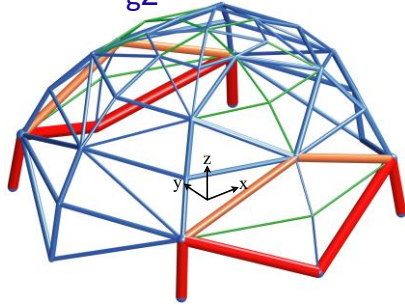
Reduced drift ratios of the optimized structure result in decreased likelihood of exceeding the threshold value

Drift Ratio Time History

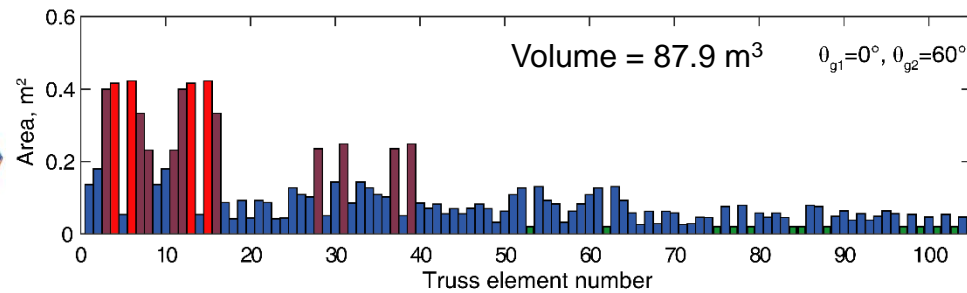
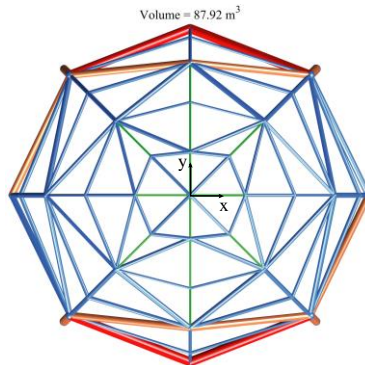
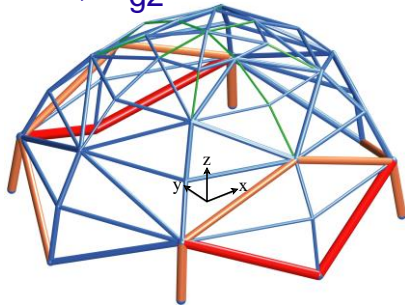


Two directional ground components of earthquake ground excitations: optimal bar areas

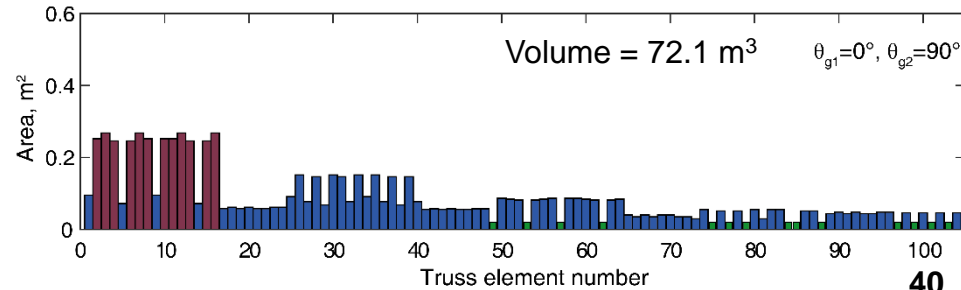
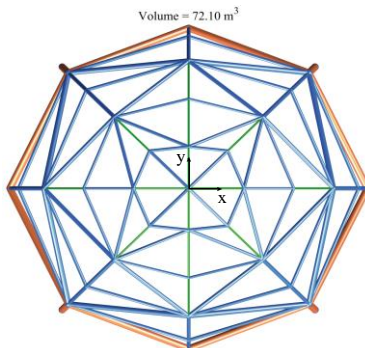
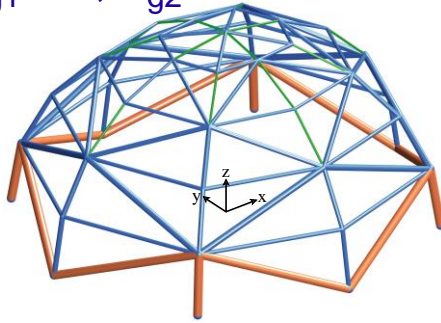
$\theta_{g1}=0^\circ, \theta_{g2}=30^\circ$



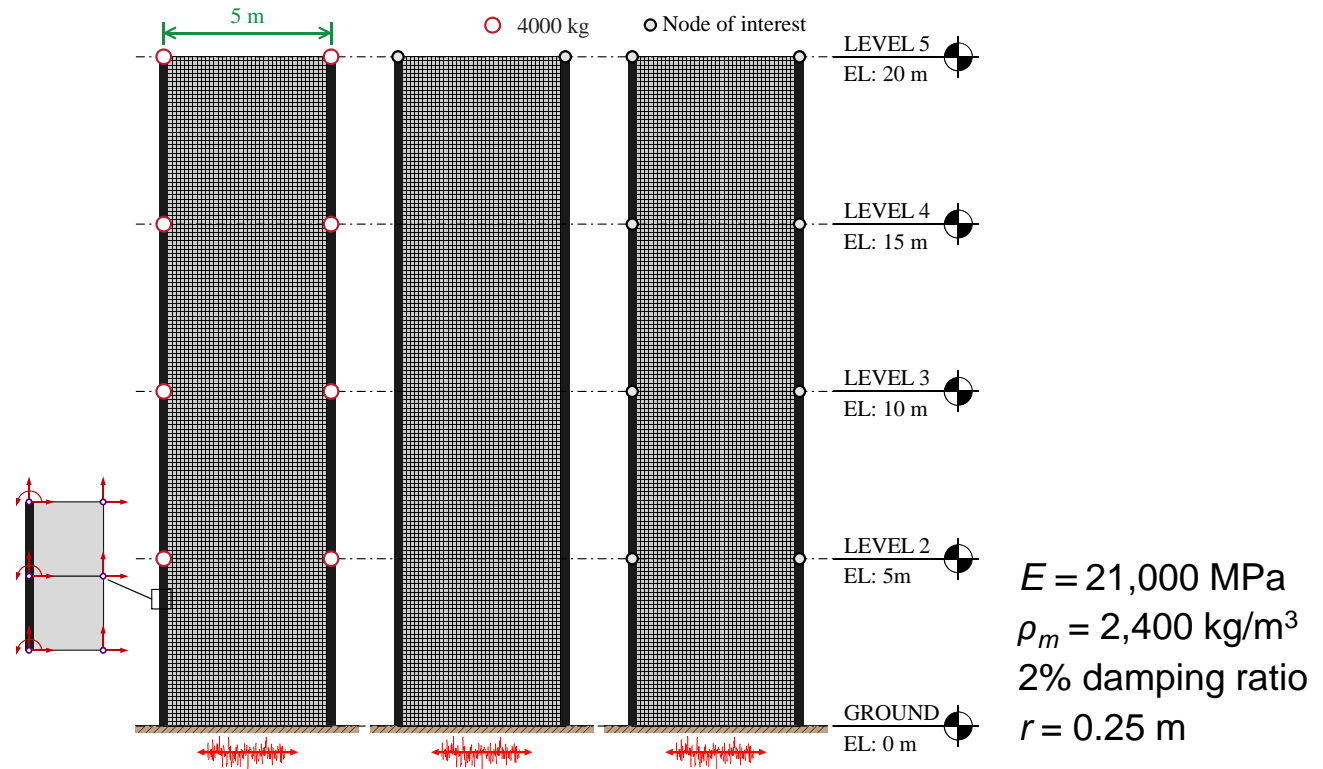
$\theta_{g1}=0^\circ, \theta_{g2}=60^\circ$



$\theta_{g1}=0^\circ, \theta_{g2}=90^\circ$



Topology optimization can identify the optimal bracing layout of a structure



min ρ volume

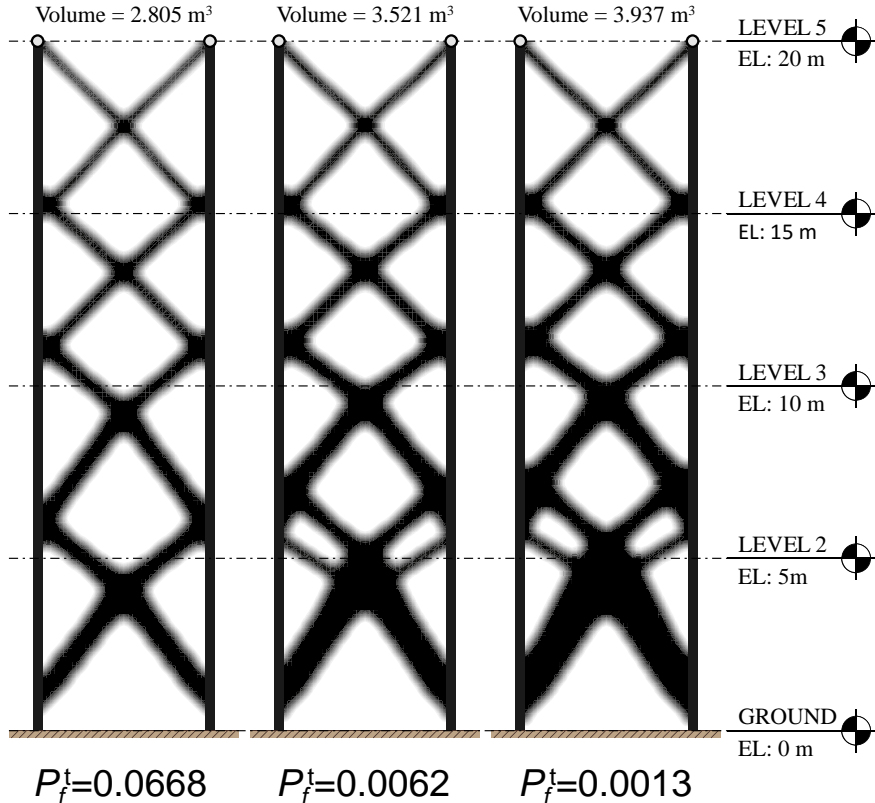
s.t $P_{fp}(g) \leq P_f^{\text{target}}$

$\varepsilon \leq \rho \leq 1.0$

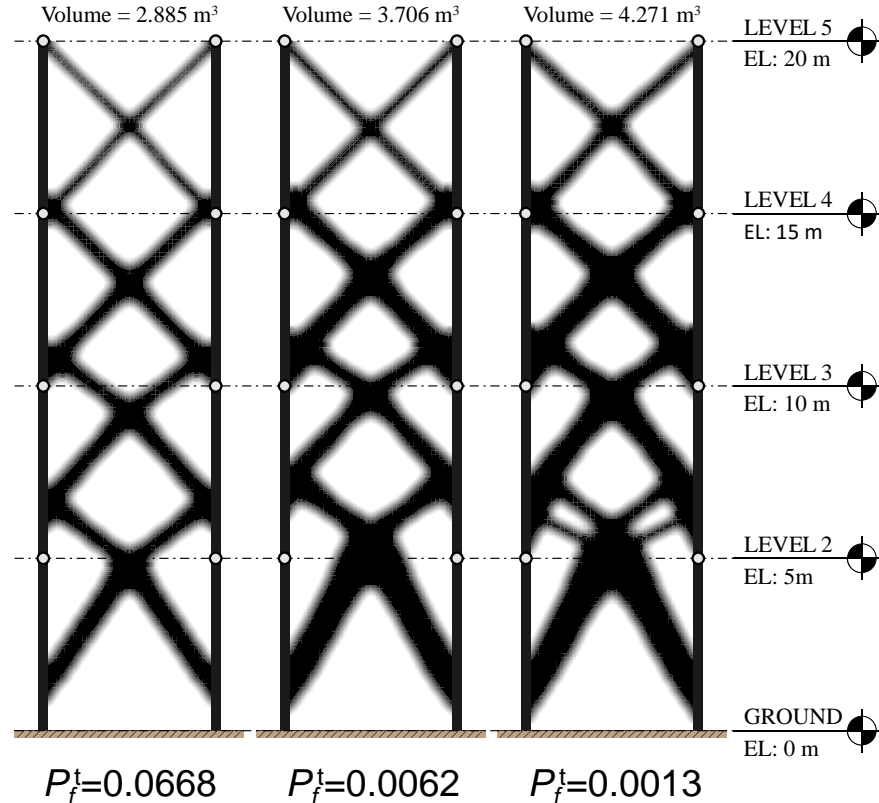
with $\mathbf{M}(\rho)\ddot{\mathbf{u}}(t, \rho) + \mathbf{C}(\rho)\dot{\mathbf{u}}(t, \rho) + \mathbf{K}(\rho)\mathbf{u}(t, \rho) = -\mathbf{M}(\rho)\mathbf{l}f(t)$

Reliable bracing systems can be interpreted from optimal topologies

Tip Displacement Constraint



Inter-story Drift Constraint



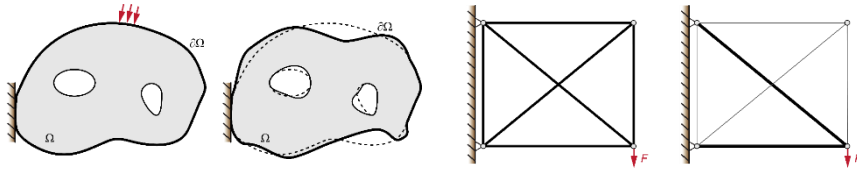
Optimization shows that **reinforcing lower regions** will efficiently control the **tip displacement**, whereas adjusting **each bracing module** will lead to successful designs of structures fulfilling **inter-story drift** ratio criteria

Stochastic design and topology optimization remarks

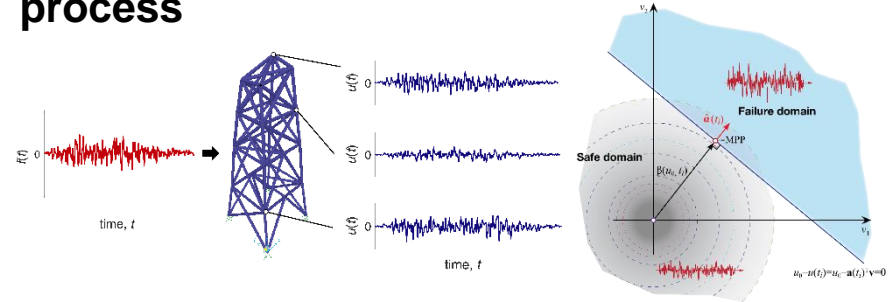
- ❑ **New optimization framework** was proposed to incorporate the first passage probability into size optimization and topology optimization of structures
- ❑ **Parameter sensitivity formulation** of the probabilistic constraint on the first passage probability was derived
- ❑ **Lateral bracing system** of structures subjected to stochastic ground motions was optimized to identify optimal member sizes under engineering constraints associated with structural design criteria
- **Different types of failure events** such as different time points and locations as well as multiple design criteria can be considered
- Optimization frameworks under **non-stationary** stochastic processes in **time domain** as well as in **frequency domain** need to be further studied

Presentation outline

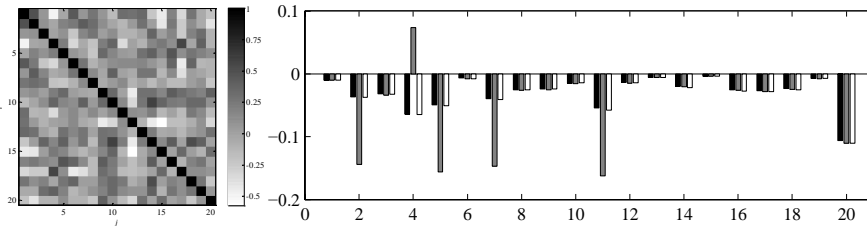
1. Introduction



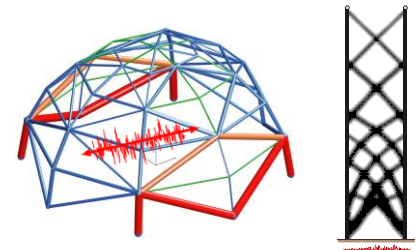
2. Discrete representation of stochastic process



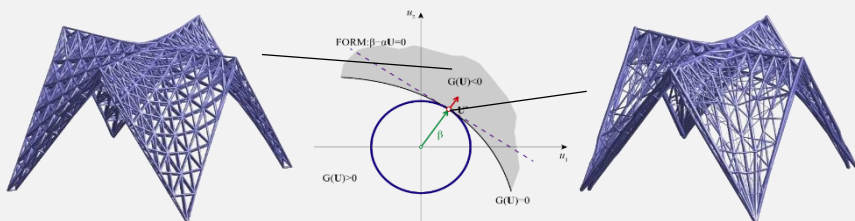
3. Parameter sensitivity of system reliability



4. Structural design and topology optimization under stochastic excitations



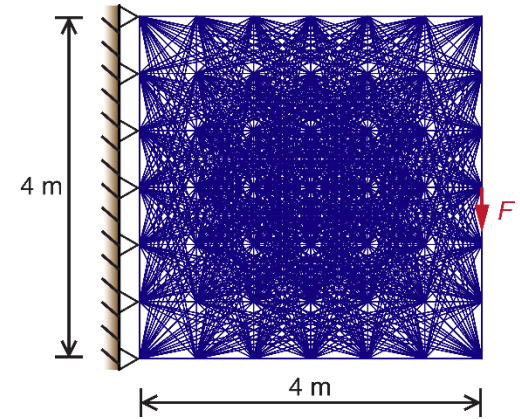
5. Reliability-based topology optimization by ground structure method



Determination of a proper cut-off value is ambiguous in conventional filter

□ Elastic formulation

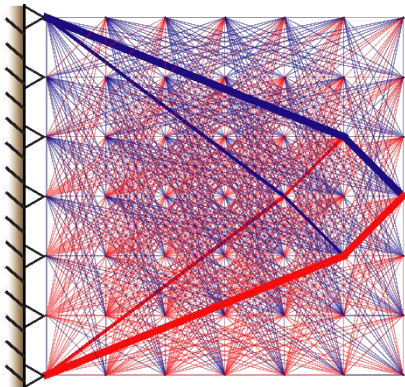
$$\begin{aligned} \min_{\mathbf{A}} \quad & C = \mathbf{f}^T \mathbf{u}(\mathbf{A}) \\ \text{s.t.} \quad & \mathbf{L}^T \mathbf{A} \leq V_s \\ & \mathbf{A}^{lower} \leq \mathbf{A} \leq \mathbf{A}^{upper} \\ \text{with} \quad & \mathbf{K}(\mathbf{A}) \mathbf{u}(\mathbf{A}) = \mathbf{f} \end{aligned}$$



Ground structure

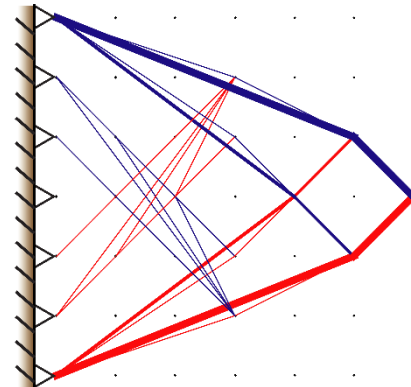
□ Filter

$$A_i = \begin{cases} 0 & \text{if } A_i / \max(\mathbf{A}) < \varepsilon_{\text{cut-off}} \\ A_i & \text{otherwise} \end{cases}, \quad 0 \leq \varepsilon_{\text{cut-off}} \leq 1$$



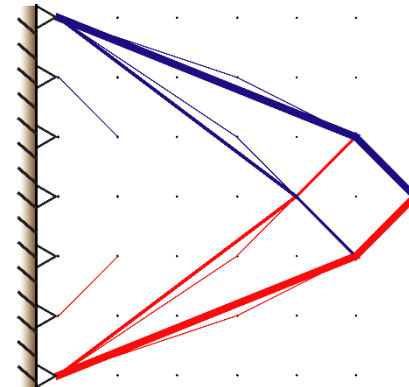
$\varepsilon_{\text{cut-off}} = 0.0$

- Impractical structure



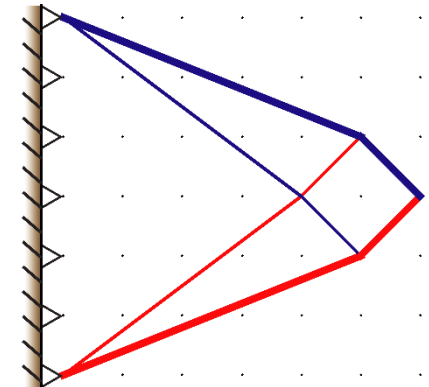
$\varepsilon_{\text{cut-off}} = 0.0001$

- Many thin bars



$\varepsilon_{\text{cut-off}} = 0.001$

- Hanging bars
- Internal mechanism



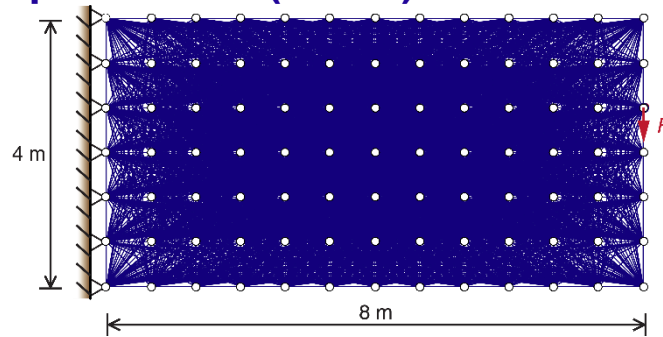
$\varepsilon_{\text{cut-off}} = 0.1$

- Feasible structure

Conventional filtering approach may lead to the violation of the prescribed target failure probability

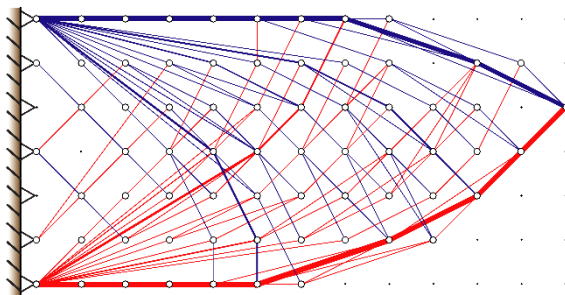
Reliability-based topology optimization (RBTO)

$$\begin{aligned} & \min_{\mathbf{d}, \mu_{\mathbf{X}}} f(\mathbf{d}, \mu_{\mathbf{X}}) \\ & \text{s.t.} \quad P_f[g(\mathbf{d}, \mathbf{X}) \leq 0] \leq P_f^{\text{target}} \\ & \quad \mathbf{d}^{\text{lower}} \leq \mathbf{d} \leq \mathbf{d}^{\text{upper}} \\ & \text{with } \mathbf{K}(\mathbf{d})\mathbf{u}(\mathbf{d}, \mathbf{X}) = \mathbf{f}(\mathbf{X}) \end{aligned}$$

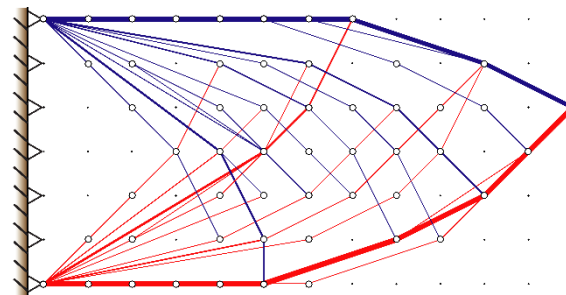


Ground structure

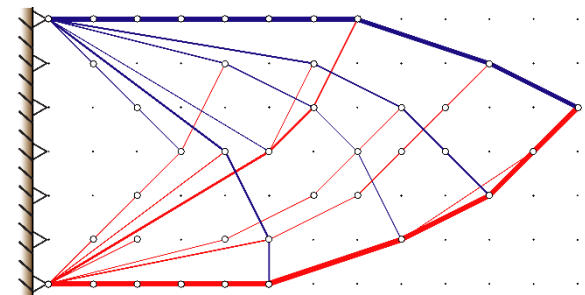
Objective: minimize volume, Constraint: compliance ($P_f^{\text{target}}=0.005$)



$\epsilon_{\text{cut-off}} = 0.0001$



$\epsilon_{\text{cut-off}} = 0.01$



$\epsilon_{\text{cut-off}} = 0.05$

Conventional filtering method

| | ϵ_{cutoff} | | | |
|--------------------|----------------------------|-----------------------|-----------------------|-----------------------|
| | 0.05 | 0.01 | 0.0001 | 0.000001 |
| Volume | 369.777 | 384.323 | 386.480 | 386.489 |
| $P_{f\text{FORM}}$ | 1.00 | 7.95×10^{-3} | 5.01×10^{-3} | 5.00×10^{-3} |
| $P_{f\text{MCS}}$ | 1.00 | 8.12×10^{-3} | 5.09×10^{-3} | 5.07×10^{-3} |

Discrete filtering scheme enables filtering of well-defined structures from ground structures

□ Optimization formulation (compliance)

$$\begin{aligned} \min_{\mathbf{A}} \quad & \mathbf{f}^T \mathbf{u}(\mathbf{A}) \\ \text{s.t.} \quad & \sum_{i=1}^{ne} A_i L_i \leq V_c \\ & \mathbf{0} \leq \mathbf{A} \leq \mathbf{A}^{upper} \end{aligned}$$

$$\text{with } \mathbf{A} = \text{Filter}(\mathbf{A}, \alpha_f) \text{ and } \min_{\mathbf{u}} \Pi(\mathbf{u}(\mathbf{A})) + \frac{\lambda}{2} \mathbf{u}(\mathbf{A})^T \mathbf{u}(\mathbf{A})$$

□ Discrete filter approach

$$\text{Filter}(\mathbf{A}, \alpha_f) = \begin{cases} 0 & \text{if } A_i / \max(\mathbf{A}) < \alpha_f \\ A_i & \text{otherwise} \end{cases}, \quad 0 \leq \alpha_f \leq 1$$

- Filter application during optimization
- Removal of critical members for equilibrium
- Detection of global equilibrium of a filtered structure
- Solution for singular systems of equations

□ Regularized potential energy (Tikhonov regularization)

$$\min_{\mathbf{u}} \Pi(\mathbf{u}) + \frac{\lambda}{2} \mathbf{u}^T \mathbf{u} \quad \frac{\partial \Pi(\mathbf{u})}{\partial \mathbf{u}} = (\mathbf{K} + \lambda \mathbf{I}) \mathbf{u} - \mathbf{f} = 0 \quad \longrightarrow \quad \mathbf{u}_p = (\mathbf{K} + \lambda \mathbf{I})^{-1} \mathbf{f}$$

□ Global equilibrium error

$$\frac{\|\mathbf{K} \mathbf{u}_p - \mathbf{f}\|}{\|\mathbf{f}\|} \leq \gamma (= 10^{-4})$$

Double loop RBTO: an outer loop for optimization and an inner loop for the reliability analysis

□ Double-loop RBTO

$$\begin{array}{l} \min_{\mathbf{d}, \boldsymbol{\mu}_x} f(\mathbf{d}, \boldsymbol{\mu}_x) \\ \text{s.t.} \quad P_f[g(\mathbf{d}, \mathbf{X}) \leq 0] \leq P_f^{\text{target}} \\ \quad \mathbf{d}^{\text{lower}} \leq \mathbf{d} \leq \mathbf{d}^{\text{upper}} \\ \text{with } \mathbf{K}(\mathbf{d})\mathbf{u}(\mathbf{d}, \mathbf{X}) = \mathbf{f}(\mathbf{X}) \end{array}$$

- Two nested optimization loops
- 1) Design optimization: outer loop
 - 2) Reliability assessment: inner loop

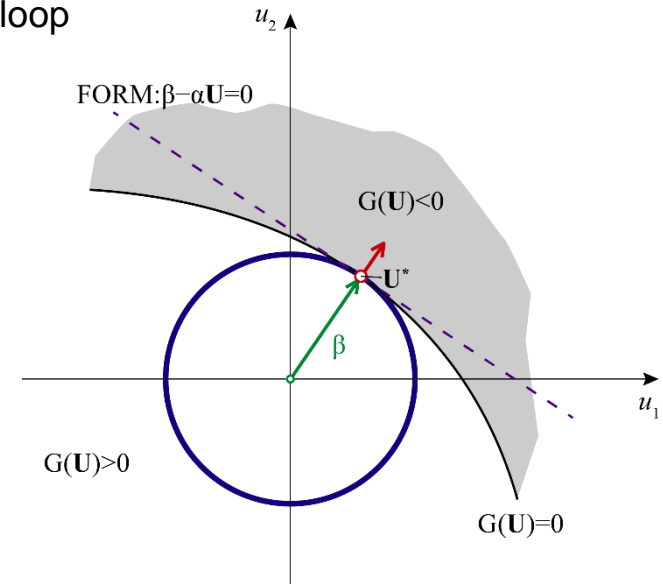
□ Failure probability (FORM: Der Kiureghian, 2005)

$$P_f = \int_{g(\mathbf{X}) \leq 0} f(\mathbf{x}) d\mathbf{x} = \int_{G(\mathbf{u}) \leq 0} \varphi_n(\mathbf{u}; \mathbf{l}) d\mathbf{u} \cong \Phi[-\beta]$$

□ Performance Measure Approach (PMA)

$$\begin{array}{l} \min_{\mathbf{d}, \boldsymbol{\mu}_x} f(\mathbf{d}, \boldsymbol{\mu}_x) \\ \text{s.t.} \quad g^{\text{PMA}}(\mathbf{d}, \mathbf{U}) \equiv g_{P_f^{\text{target}}} \geq 0 \\ \quad \mathbf{d}^{\text{lower}} \leq \mathbf{d} \leq \mathbf{d}^{\text{upper}} \\ \text{with } \mathbf{K}(\mathbf{d})\mathbf{u}(\mathbf{d}, \mathbf{X}) = \mathbf{f}(\mathbf{X}) \end{array}$$

$$g^{\text{PMA}}(\mathbf{d}, \mathbf{U}) = \arg \min \left\{ G(\mathbf{d}, \mathbf{U}) \mid \|\mathbf{U}\| = \beta^{\text{target}} \left(= -\Phi^{-1}[P_f^{\text{target}}] \right) \right\}$$



FORM approximations for a component problem

Efficiency in RBTO can be improved by the reliability analysis loop by a non-iterative procedure

□ KKT optimality condition

$$\nabla_{\mathbf{U}}G(\mathbf{d},\mathbf{U})+\lambda \cdot \nabla_{\mathbf{U}} \left(\|\mathbf{U}\| - \beta^{\text{target}} \right) = \mathbf{0}$$

From the geometric interpretation

$$\lambda \geq 0$$

Assume $\nabla H = 2\mathbf{U}$

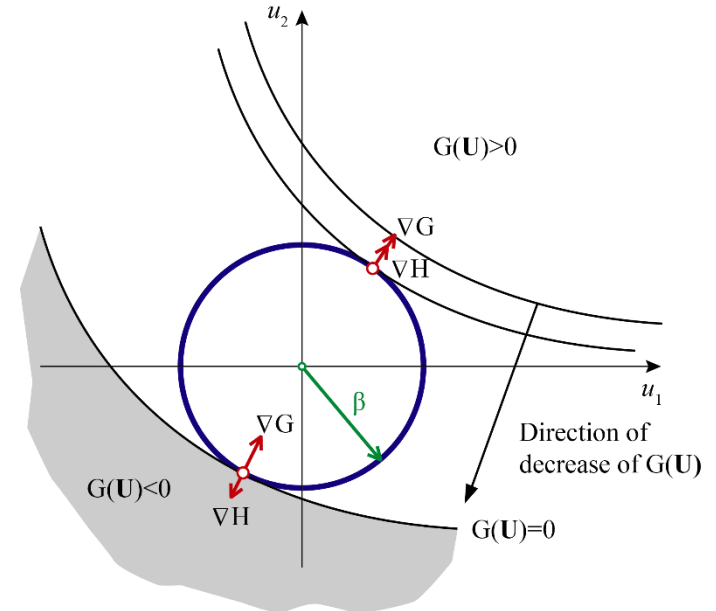
$$\mathbf{U}^* = \mathbf{U} = - \frac{\|\nabla_{\mathbf{U}}G(\mathbf{d},\mathbf{U})\|}{2\lambda} \cdot \frac{\nabla_{\mathbf{U}}G(\mathbf{d},\mathbf{U})}{\|\nabla_{\mathbf{U}}G(\mathbf{d},\mathbf{U})\|} \quad \beta^{\text{target}} = \frac{\|\nabla_{\mathbf{U}}G(\mathbf{d},\mathbf{U})\|}{2\lambda}$$

Since $\|\mathbf{U}\| = \beta^{\text{target}}$

□ Single-loop RBTO using discrete filter

$$\begin{aligned} \min_{\mathbf{A}} \quad & f(\mathbf{A}) \\ \text{s.t.} \quad & g^{\text{Single}}(\mathbf{A}, \mathbf{X}(\mathbf{U}^t)) \geq 0 \\ & \mathbf{0} \leq \mathbf{A} \leq \mathbf{A}^{\text{upper}} \end{aligned}$$

$$\text{with } \mathbf{A} = \text{Filter}(\mathbf{A}, \alpha_f) \quad \text{and} \quad \min_{\mathbf{u}} \Pi(\mathbf{A}(\mathbf{d}, \mathbf{X}(\mathbf{U}^t))) + \frac{\lambda}{2} \mathbf{u}(\mathbf{A}, \mathbf{X}(\mathbf{U}^t))^T \mathbf{u}(\mathbf{A}, \mathbf{X}(\mathbf{U}^t))$$



Geometric presentation of optimal solution (one active constraint).

Application of the proposed method in a large structure to identify the optimal topology with a desired reliability

□ Optimization problem

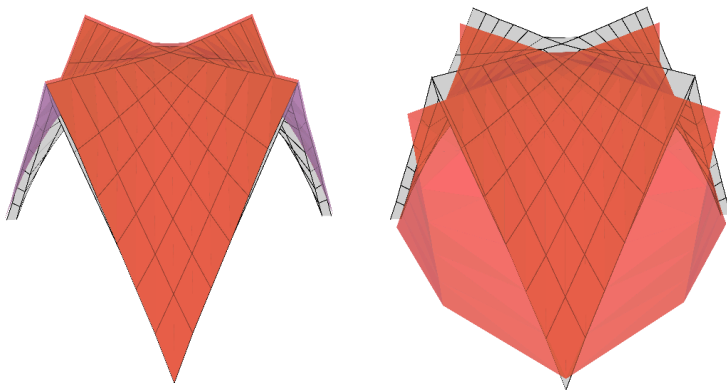
$$\min_{\mathbf{A}} \text{Volume}$$

$$\text{s.t. } P_f(\text{10-Compliance}) \leq 0.0025$$

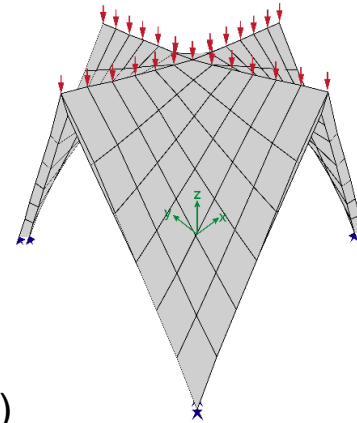
$$\mathbf{0} \leq \mathbf{A} \leq \mathbf{A}^{upper}$$

$$\text{with } \mathbf{A} = \text{Filter}(\mathbf{A}, \alpha_f)$$

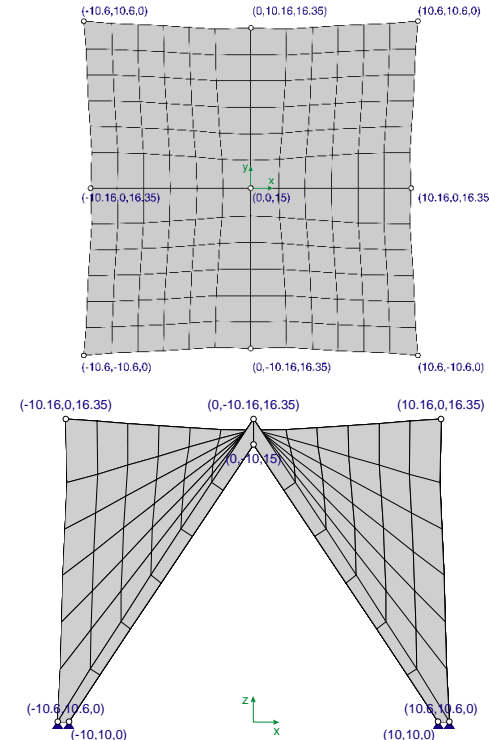
$$\text{and } \min_{\mathbf{u}} \Pi(\mathbf{A}(\mathbf{d}, \mathbf{X}(\mathbf{U}^t))) + \frac{\lambda}{2} \mathbf{u}(\mathbf{A}, \mathbf{X}(\mathbf{U}^t))^T \mathbf{u}(\mathbf{A}, \mathbf{X}(\mathbf{U}^t))$$



Restrict zones (GRAND3)



Design domain, loadings, and BCs



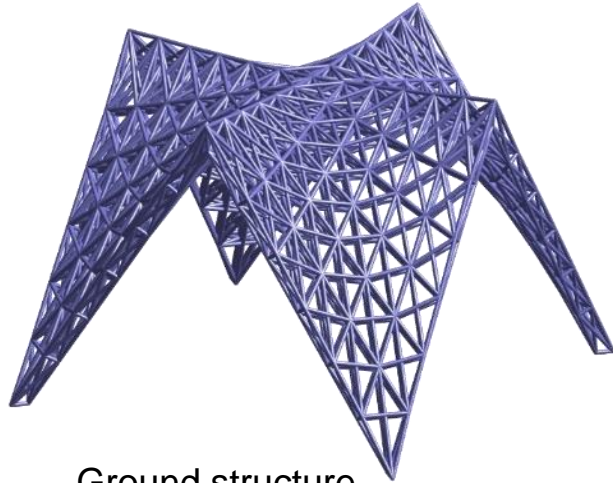
Plan & section view

Random variable: Forces, Young' Modulus

| E (GPa) | | F (kN) | | C_{max} | P_f^{target} | α_f | A^{upper} (m ²) |
|------------|---------------|------------|---------------|-----------|----------------|------------|-------------------------------|
| μ_{mE} | σ_{sE} | μ_{mF} | σ_{sF} | | | | |
| 200 | 40 | 100 | 20 | 10 | 0.0025 | 0.01 | 1.5 |

Different connectivity levels result in the different topologies in optimized solutions

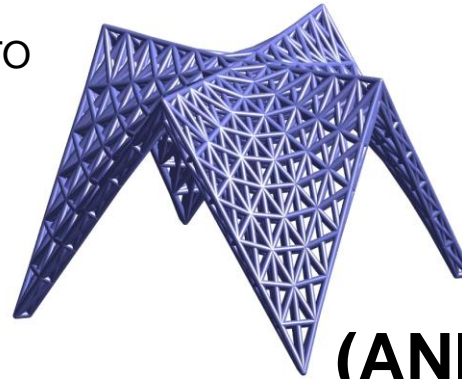
□ Connectivity Level 1



Ground structure

Iter: 0, Volume = 1679.90 m³

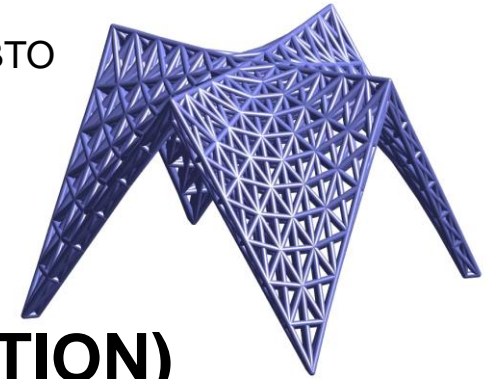
DTO



$P_{f, FORM} = 15.4\%$
Equilibrium Error=3.1e-05

Iter: 0, Volume = 1679.90 m³

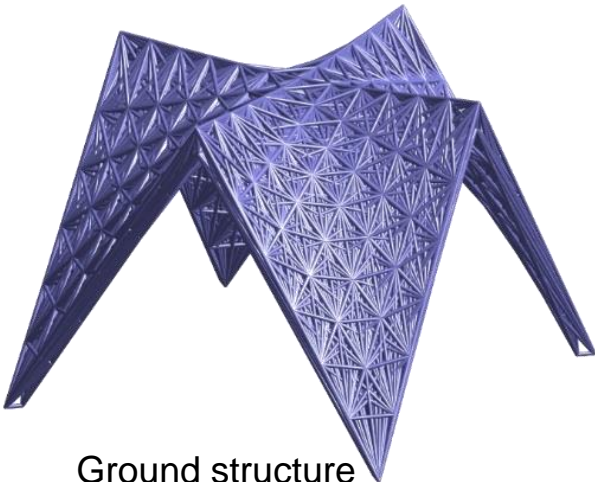
RBTO



$P_{f, FORM} = 0.0025\%$
Equilibrium Error=3.2e-05

(ANIMATION)

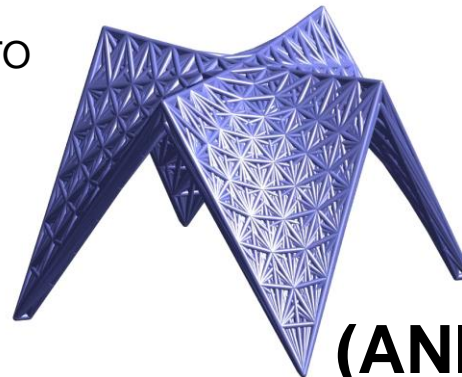
□ Connectivity Level 4



Ground structure

Iter: 0, Volume = 10780.17 m³

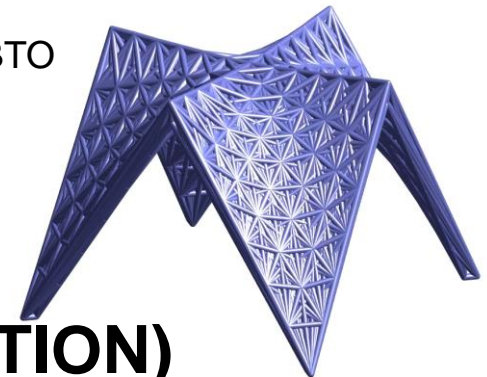
DTO



$P_{f, FORM} = 14.4\%$
Equilibrium Error=3.4e-05

Iter: 0, Volume = 10780.17 m³

RBTO

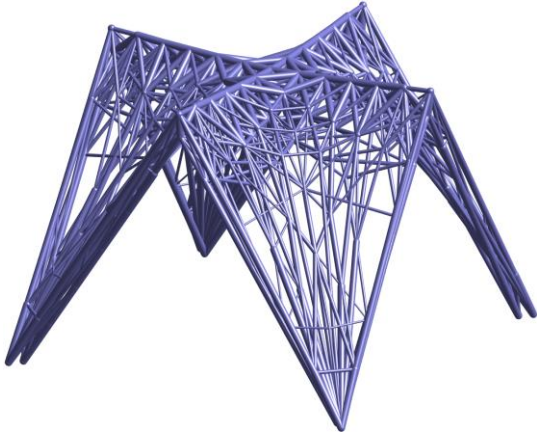


$P_{f, FORM} = 0.0025\%$
Equilibrium Error=3.4e-05

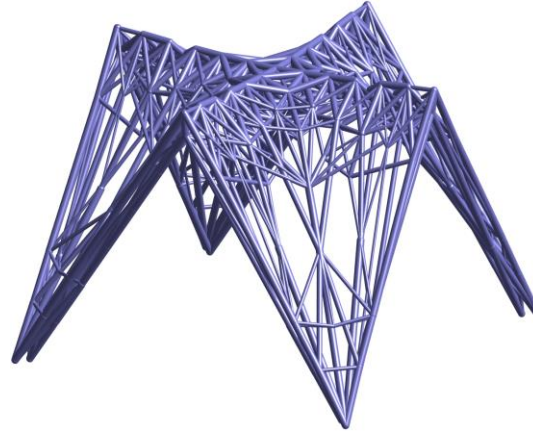
(ANIMATION)

Different filter parameters generate a variety of optimal solutions for application in engineering

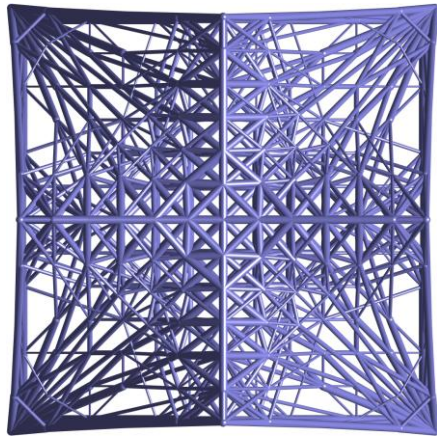
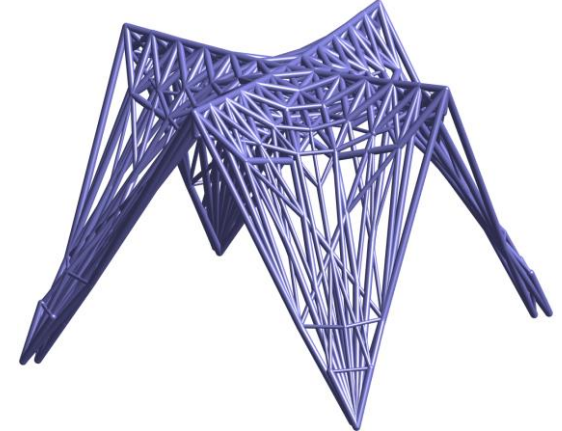
Volume = 2579 m³



Volume = 2670 m³



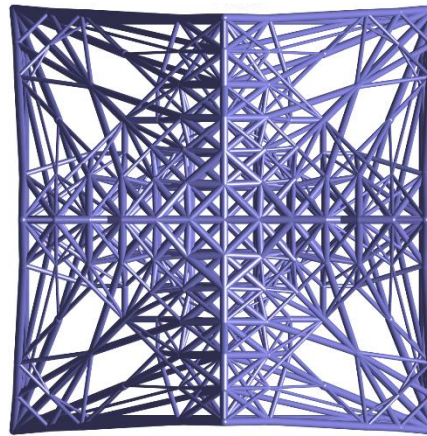
Volume = 2897 m³



$\alpha_f = 0.05$

$P_{f, \text{FORM}} = 0.0025\%$

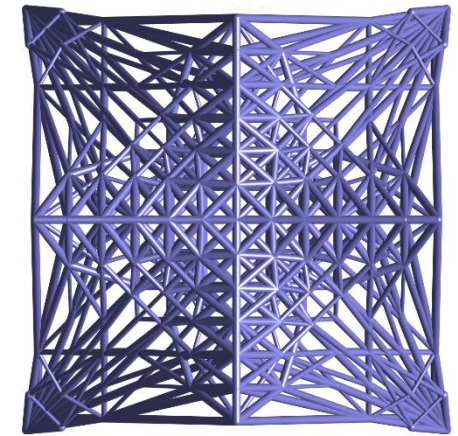
Equilibrium Error=3.1e-05



$\alpha_f = 0.075$

$P_{f, \text{FORM}} = 0.0025\%$

Equilibrium Error=3.2e-05



$\alpha_f = 0.09$

$P_{f, \text{FORM}} = 0.0025\%$

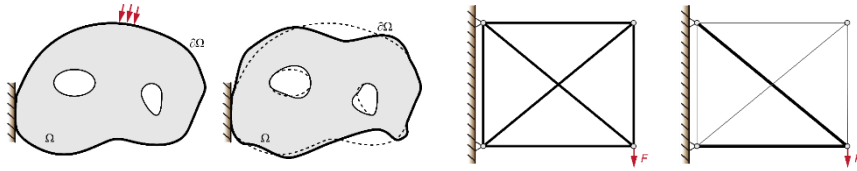
Equilibrium Error=3.2e-05

RBTO employing the discrete filter remarks

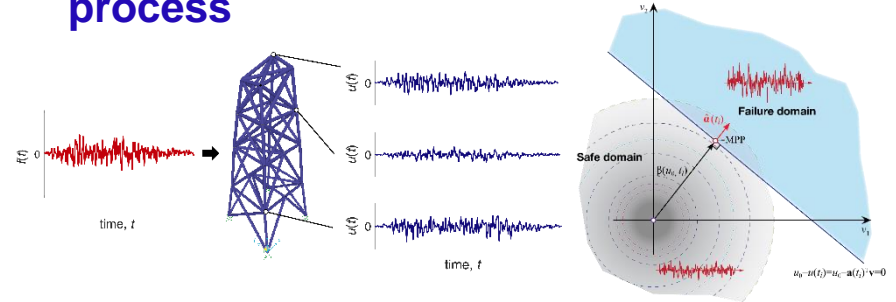
- ❑ The conventional filter and the discrete filter were reviewed
- ❑ The framework of single-loop RBTO employing the discrete filtering scheme was developed
- ❑ Optimal solutions satisfying the desired failure probability and global equilibrium were obtained from the proposed method
- ❑ Various optimal solutions can be delivered with the proposed method

Summary

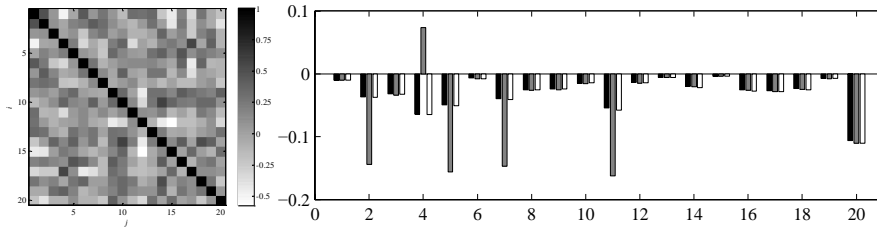
1. Introduction



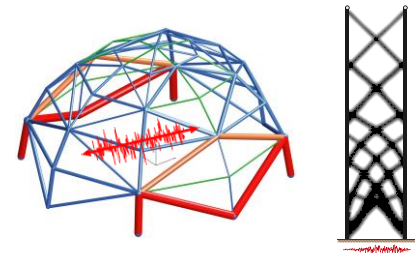
2. Discrete representation of stochastic process



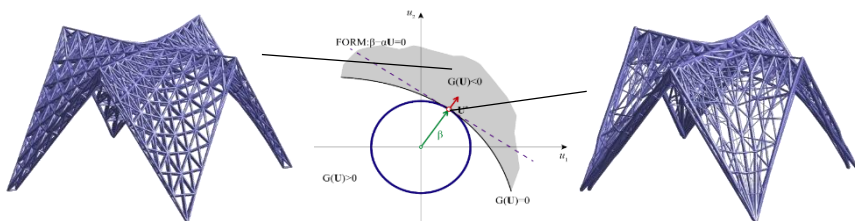
3. Parameter sensitivity of system reliability



4. Structural design and topology optimization under stochastic excitations



5. Reliability-based topology optimization by ground structure method



Acknowledgment



University of Illinois, Urbana-Champaign



Dr. Paulino's research group



Dr. Song's research group



National Science Foundation (NSF) : CMMI 1234243

Thank you

